Vietnam Journal of Earth Sciences, 46(2), 168-201, https://doi.org/10.15625/2615-9783/20053

Vietnam Journal of Earth Sciences
https://vjs.ac.vn/index.php/jse

Evaluation of the Neogene depositional dynamics in the Malay-Tho Chu Basin based on seismic analysis: effects of local and regional tectonism and paleoclimatic variations

Tu-Anh Nguyen[1], Michael B.W. Fyhn*[2], Lars O. Boldreel[1], Ioannis Abatzis[2], Huyen T. Nguyen[3]

[1]*Institute of Geoscience and Natural Resources, University of Copenhagen, Øster Voldgade 10, 1350 Copenhagen K, Denmark*
[2]*Geological Survey of Denmark and Greenland, GEUS, Øster Voldgade 10, 1350 Copenhagen K, Denmark*
[3]*Vietnam Petroleum Institute (VPI), 167 Trung Kinh Street, Yen Hoa, Cau Giay, Hanoi, Vietnam*

Received 16 August 2023; Received in revised form 15 December 2023; Accepted 31 January 2024

ABSTRACT

Depositional environments in areas located near sea level are vulnerable to even subtle changes in both tectonism, climate and eustatic sea level. Sorting out mechanisms behind depositional changes in inner shelf-margins and epeiric seas is therefore far from straight forward. The epeiric Malay-Tho Chu Basin, located in the shallow Gulf of Thailand offshore Vietnam, contains a thick uppermost Oligocene to Recent post-rift succession. Based on 18000 km of 2D seismic profiles, the uppermost Oligocene-Recent succession is subdivided into six seismic sequences. Seismic facies mapping of each sequence complemented by information from industry completion reports of 14 wells document a gradual increase in marine influence from latest Oligocene through Middle Miocene time. The increased marine influence reflects the propagation and opening of the southwestern spreading arm of the East Vietnam Sea (South China Sea (East Sea)) combined with rapid subsidence in the Malay-Tho Chu Basin resulting from fast thermal relaxation following Oligocene rifting and amplified by mild fault-controlled subsidence in especially the western part of the area. From the latest Middle Miocene, slowed subsidence and regression occurred in association with uplift in the nearby southwestern East Vietnam Sea. From the latest Miocene, and during the Pliocene and Pleistocene, subsidence rates increased promoting marine conditions towards the East Vietnam Sea in the southeast. Meanwhile, Mekong River avulsion combined with hinterland uplift stimulated fluvial and alluvial deposition in the northern and western parts of the basin. The long-term depositional pattern was controlled primarily by tectonics, drainage evolution and climate. Meanwhile, flood- and delta plain deposits intercalated with stacked fluvial incisions, often filled by estuarine deposits, document short-lived environmental changes most likely controlled by eustatic sea level fluctuations. Such intervals developed during latest Middle Miocene to Pleistocene periods of slow subsidence or fast depositional rates and are interpreted to be the result of substantial eustatic sea level fluctuations.

Keywords: Malay-Tho Chu Basin, depositional environments, regional tectonism, paleoclimate, sea level changes, 2D seismic, East Vietnam Sea, Gulf of Thailand.

1. Introduction

Shallow shelfs and epicontinental seas cover much of Earth's surface, and the related deposits make up a large fraction of the geological sedimentary record. The depositional environment in such settings is vulnerable to even subtle changes in boundary conditions, and even small variations in

*Corresponding author, Email: mbwf@geus.dk

tectonism, climate and sea level may cause substantial shifts in depositional environment (e.g. Macdonald, 1991; Browning et al., 2009; Jaillard et al., 2019). Disentangling the mechanisms controlling deposition of sedimentary sections from such setting tends to be highly complicated. This applies especially to basins formed in regions of active tectonism and in times with rapidly evolving climate and sea level.

The Gulf of Thailand is underlain by such basins (Pubellier and Morley, 2014; Morley and Racey, 2016). Formed during the Cenozoic in a region characterized by hinterland uplift, the establishment of modern SE Asian rivers, opening of the East Vietnam Sea (South China Sea (East Sea)) and the rise of the Himalaya and Tibetan Plateau (Briais et al., 1993; Carter et al., 2000; Clift, 2006; Clift and Sun, 2006; Clift et al., 2008; Fyhn et al., 2016; 2023; Miao et al., 2017), these basins likely experienced pronounced variations in climate, hinterland weathering, sediment supply, marine influence and sea level fluctuations.

The Malay-Tho Chu Basin (MLTCB) is located in the Vietnamese part of the Gulf of Thailand (Fig. 1a) bounded to the west by territorial waters of Malaysia, Thailand and Cambodia and by the East Vietnam Sea to the east. It contains a Cenozoic depositional record of hinterland uplift and erosion, changing tectonic phases in Indochina, climatic variations and sea level fluctuations (Fyhn et al., 2010a; b; Petersen et al., 2009; 2011). During the Neogene, the MLTCB developed as a post-rift basin located on the shallow to subaerially exposed, inner shelf in the vicinity of the present outlet of the Mekong and Chao Phraya rivers that drains most of greater Indochina. This makes the basin ideally suited for studying the influence of tectonism, regional climate, avulsion, and relative sea level fluctuations on deposition.

Based on seismic facies analyses of a regional 2D seismic grid covering around 40,000 km^2 integrated with information from completion well reports, this study interprets the latest Oligocene and Neogene gross depositional evolution of the MLTCB in context with the regional tectonic, climatic and fluctuating eustatic sea level history. The aim of the study is to illustrate how deposition developed in an inner shelf basin during a period with substantial climatic variation, eustatic sea level fluctuations, major river avulsion and a rapidly evolving regional tectonic setting, and how tectonism, Mekong River avulsion and climate exerted the primary control on long-term deposition, while repeated eustatic sea level fluctuations only resulted in short-lived changes in depositional environment.

2. Study area

2.1. Geological setting

The MLTCB corresponds to the Vietnamese part of the Malay and the Khmer basins (Fyhn et al., 2010a) (Fig. 1a) situated in the northeastern Gulf of Thailand and next to the East Vietnam Sea. The area is characterized by a long and complex geological history, and the basin is floored by a complex mosaic of Paleozoic and Mesozoic sediments and igneous rocks (Fyhn et al., 2016; Nguyen et al., 2021; Wait et al., 2021). The MLTCB was formed by Middle or Late Eocene to Oligocene rifting possibly related to left-lateral transtension, followed by Neogene post-rift subsidence and moderate fault reactivation (Fyhn et al., 2010a; Smith et al., 2007; Tapponnier et al., 1986; Tjia, 1994). The NW-SE trend of the MLTCB reflects the structural outline established during the Eocene - Oligocene rifting and was studied by Fyhn et al. (2010a).

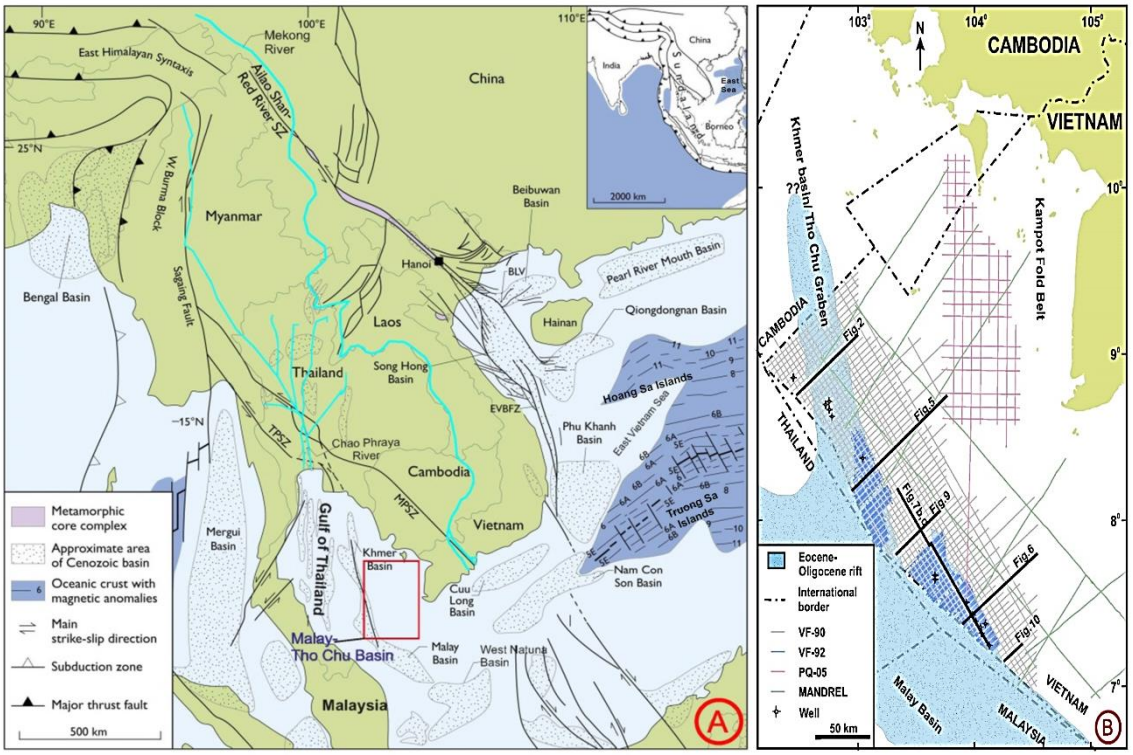

Figure 1. A: Overview map of Indochina and the East Sea, the red square indicates the study area. Modified after Nytoft et al. (2020). B: Map illustrating the study area and the location of seismic profiles together with wells, international borders and basins. Modified after Fyhn et al. (2010b)

During Eocene and Oligocene time, the Paleogene rift system developed in the southwestern part of the study area (Fig. 2) (Fyhn et al., 2010a). In contrast, the northeastern part constituted an elevated rift shoulder (Fyhn et al., 2010a, b). A series of deep grabens and half-grabens formed during this period in the southwest, which were filled by mainly continental, but possibly also some shallow marine sediments (Fyhn et al., 2010a; Petersen et al., 2009; 2011).

Extension slowed towards the latest Oligocene-earliest Miocene and thermal sagging dominated throughout the Neogene in many basins along the Indochina margin including the MLTCB (Tjia, 1994; Fyhn et al., 2009; 2010a; 2018, Pubellier and Morley, 2014; Smith et al., 2019). In the MLTCB, subsidence broadened to encompass formerly elevated areas resulting in gradual burial of structural highs (Fyhn et al., 2010a). However, moderate Miocene extension reactivated Paleogene rift structures in the western part of the MLTCB in particular (Fyhn et al., 2010a). This reactivation was attributed to the continuation of rifting in the western Gulf of Thailand (Fyhn et al., 2010a; Morley, 2017; Phoosongsee et al., 2019).

Inversion affected many basins around Indochina, including the nearby West Natuna, Cuu Long and Malay Basins (Ginger et al., 1994; Olson and Dorobek, 2000; Pubellier and Morley, 2014; Fyhn and Phach, 2015; Fyhn et al., 2018; Smith et al., 2019; Rizzi et al., 2020; Hoang et al., 2020; 2023). In the Malay Basin, inversion

occurred from the Middle Miocene lasting to the mid-Pliocene (Madon, 2007; Olson and Dorobek, 2000; Pubellier and Morley, 2014) and erosion pulses associated with inversion-related uplift affected the central part of the basin (Hutchison, 1996; Ngah et al., 1996; Madon, 1997; Morley and Westaway, 2006).

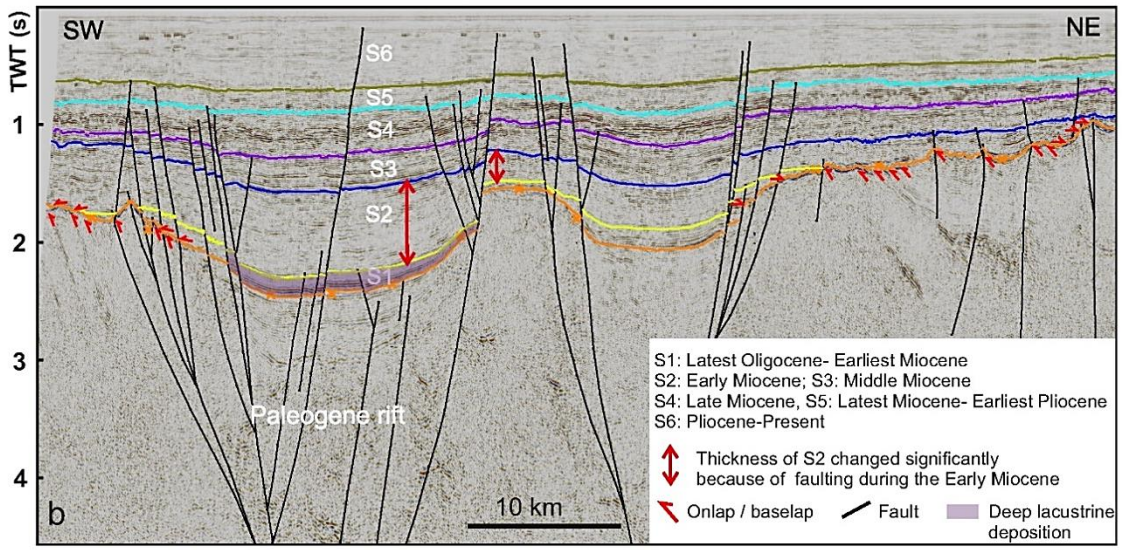

Figure 2. Seismic profile illustrating the six uppermost Oligocene to Recent sequences in the Malay-Tho Chu Basin. Red arrows indicate the significant changes in thickness of S2 caused by Early Miocene faulting. Location shown on Fig. 1

In the East Vietnam Sea, seafloor spreading started during the Early Oligocene offshore South China (Taylor and Hayes, 1983; Briais et al., 1993; Li et al., 2014). Following latest Oligocene southwards jump of the seafloor spreading center, the southwestern East Vietnam Sea sub-basin started to open (Barckhausen et al., 2014; Li et al., 2014). The southwestern spreading center propagated southwestwards towards the Gulf of Thailand opening the southwestern East Vietnam Sea sub-basin during the Early Miocene. Subsequently, seafloor spreading completed during either the middle Early or latest Early Miocene (Barckhausen et al., 2014; Li et al., 2014).

A significant unconformity dated roughly 12 to 9 Ma formed in response to uplift, erosion and non-deposition in the area located southwest of the southwestern East Vietnam Sea spreading center (Matthews et al., 1997; Dung et al., 2018). A large part of the Middle-Upper Miocene is therefore missing in Nam Con Son and the Cuu Long Basins (Morley et al., 2019). During the same time, the Malay Basin experienced slow subsidence rates, which resulted in the development of a very thick and widely distributed coal seam in the south of the MLTCB (Robert Morley pers.com., 2019), and in the West Natuna Basin, the Late Miocene is represented by a hiatus reflecting inversion and uplift (Morley, 2012).

Following the uplift, fast subsidence and rapid deposition led to thick accumulations of Upper Miocene to Pleistocene deposits in the Cuu Long and Nam Con Son basins (Clift and Wilson, 2023). Comparable increases in terrigenous sediment accumulation since the Late Neogene occurred over most of the Indochina margin (Mathews et al., 1997; Lee et al., 2001; Fyhn et al., 2009a; 2013; 2023; Dung et al., 2018).

Clift and Sun (2006) linked high Pliocene-Quaternary sedimentation rates with hinterland uplift and rapid weathering forced by SE Asia monsoon strengthening. A partly related mechanism was proposed for the increase in sedimentation and subsidence rates southeast of Vietnam with a significant increase in sediment delivery occurring from the Mekong River driven by both river avulsion, enhanced summer monsoon and denudation of southern Indochina (Clift & Wilson, 2023).

2.2. Sea-level changes and Southeast Asian paleoclimate since the latest Oligocene

The Oligocene-Recent is characterized by the evolving icehouse conditions on Earth that greatly impacted eustatic sea level and climate globally as well as regionally in SE Asia (Morley, 2012; Morley et al., 2019; Miller et al., 2020). The evolving climate and fluctuating sea level affected deposition on the SE Asian shelves (Clift and Sun, 2006; Dung et al., 2018).

The eustatic sea level since the latest Oligocene is characterized by high-frequent oscillations with sea level shifts in the order of tens to more than 100 meters occurring over thousands to tens of thousands of years (Miller et al., 2020). The high-frequent cyclicity is superimposed on intermediate term eustatic variations occurring over hundreds of thousands to few million years, but the overall long-term eustatic sea level trend since the latest Oligocene (Fig. 3) can be bracketed into five epoch characterized by:

(1) A eustatic sea-level fall at the end of the Oligocene followed by.

(2) An Early-Middle Miocene rise culminating during Mid-Miocene Climatic Optimum (Haq et al., 1987; Kominz et al., 1998; Betzler et al., 2018).

(3) A late Middle to Late Miocene fall in eustatic sea level (Haq et al., 1987) followed by a.

(4) Latest Late Miocene to earliest Pliocene sea-level rise.

(5) And finally, a fall in eustatic sea level since the Early Pliocene associated with the buildup of extensive northern hemisphere ice sheets (Miller et al., 2005; 2011; 2020).

SE Asia experienced a tropical, moist and monsoonal climate during the Early and Middle Miocene promoting ever-wet conditions in the Gulf of Thailand region culminating during the Mid-Miocene Climatic Optimum (Flower and Kennett, 1994; Clift, 2006; Morley, 2012). Following the Mid-Miocene Climatic Optimum, the monsoon weakened during the Late Miocene (Fig. 3) (Clift et al., 2008). Since the Late Miocene, the SE Asian climate cooled and became less humid culminating in the Quaternary (Liu et al., 2019). At the same time, seasonality increased from about 9 Ma in central Sundaland (Morley, 2012).

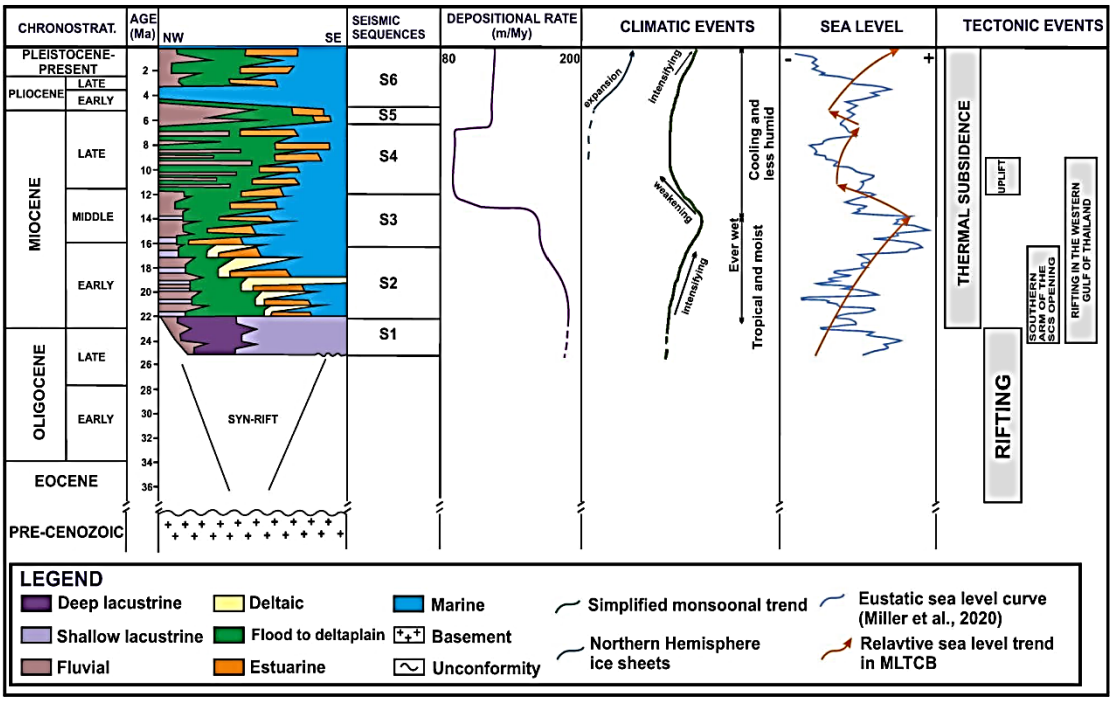

Figure 3. Summary of the latest Oligocene to Recent depositional evolution in the Malay-Tho Chu Basin. A long-term increase of marine conditions occurred from the earliest to Middle Miocene overlain by short-term relative sea-level fluctuations. Non-marine deposition increased during the latest Middle to Late Miocene. Also shown are a depositional rate curve, paleoclimatic development curve based on Clift et al. (2006) and R. Morley. (2012), eustatic sea level curve after Miller et al., 2020 and main regional tectonic events

3. Methodology and data

3.1. Dataset

The study is based on a dataset of ~18000 km of commercial 2D reflection seismic data and completion reports of 14 exploration wells. The seismic data consists of three main surveys: VF-90, VF-92 acquired by Geco on behalf of FINA Exploration and the PQ-05 seismic survey commissioned by PetroVietnam (Fig. 1b). The three main surveys cover the MLTCB in a regular grid.

The seismic surveys were collected in 1990, 1992 and 2005, respectively, using state-of-the-art techniques at the time of data acquisition and processing i.e. pre-stack time migration. Available acquisition and data information are summarized in Table 1. Survey VF-90 covers the southwestern part of the study area in a regular 4 × 4 km grid and with its 11,076 km represents approximately 60% of the total data (Fig. 1b), whereas the VF-92 survey comprises 25% of the total data and consists of infill data in the southwest. The PQ-05 survey covers the northern part of the study area and makes up around 15% of the seismic data of this study (Fig. 1b). In addition, a few regional lines belonging to the MANDREL survey (Fig. 1b) acquired in the early 1970s by Petty-Rey Geophysical were used to connect the VF-surveys with the PQ survey as well as the study area to the neighboring Cuu Long and Nam Con Son basins. Data in this study are displayed using American polarity in which positive peaks corresponding to downward impedance increases are delineated in red and troughs in blue corresponds to downward impedance decreases.

Completion reports of 14 exploration wells drilled in the MLTCB was available. Information from the reports includes summaries of biostratigraphy, information of lithology from cuttings samples enabling dating of seismic horizons and correlation of seismic facies with wells. A limited number of wireline logs from two wells was available.

Table 1. Information of seismic dataset used in this study

Survey	VF-90	VF-92	PQ-05
Operator	FINA Exporation	FINA Exporation	Petro Vietnam
Year of acquirement	1990	1992	2005
Polarity	American	American	American
Fold	24	24	80
Streamer length (m)	3000	3000	4500
Receiver interval (m)	12.5	12.5	12.5
Airgun volume (CUIns)	4804	4804	3000
Shot distance (m)	25	25	25

3.2. Methodology

The seismic interpretation was carried out using Petrel software. The uppermost Oligocene to Recent succession was divided into six seismic sequences, S1 to S6 descending in age, separated by seismic horizons depicting stratigraphic surfaces (Fig. 2). The seismic sequences were defined based on their seismic facies distinguishing them from over- and underlying sequences. Sequence boundaries were picked correlating base-sequence reflectors throughout the seismic grid and by the use of reflector terminations.

Seismic facies were mapped systematically for each of the six sequences based on the internal and external reflection geometries, internal and external lapping patterns, reflection amplitudes, frequencies and continuities. Reflection amplitudes, frequencies and continuities can be manipulated through processing, and in their absolute sense provide little information; but by using them in their relative sense, they become useful diagnostic and correlative tools of depositional styles when interpreted together with lapping pattern, external and internal reflection geometries and information from wells (e.g. Mitchum et al., 1977; Jenyon and Fitch, 1985).

The seismic sequences were correlated with information from the 14 well reports. In the absence of wireline log data from all the wells, correlations were mostly based on visual comparisons of well-seismic ties included in the reports. This permitted correlation of biostratigraphic and lithologic information from the wells with the seismic sequences, thus allowing biostratigraphic dating of the sequences correlated with the geological timescale of Gradstein et al. (2020).

Marine/non-marine conditions were determined in well reports based on the presence or absence of marine fossils, such as foraminifers, and by the palynomorph assemblages in cuttings. Lithology was also used in the reports together with biostratigraphic information to qualify the depositional environments.

The seismic facies pattern was interpreted using the well-established concepts proposed originally by e.g. Sangree and Widmeer (1997) and at the same time taking the relationships to neighboring facies associations into account. Well information also offered guidance to the depositional facies interpretation in the southwestern, drilled part of the study area. The facies interpretation was put into a geological context (ascribed to the geological environment) and in this manner, a geological model evolved depicted by six gross-depositional maps representing the uppermost Oligocene and Neogene sequences (Fig. 4a-f). The maps give an overview of the prevailing deposition during six periods and together

depict the depositional evolution of the MLTCB. The gross-depositional maps are simplifications of the exact history, illustrating the distribution of the prevailing facies types. Subordinate facies associations within sequences were interpreted and mapped and is indicated by hatch signatures overlain on the main facies association in the gross-depositional maps. Figures 5, 6 and 7 exemplify interpretation of such facies intercalations within sequences and across their boundaries based on seismic and well sections.

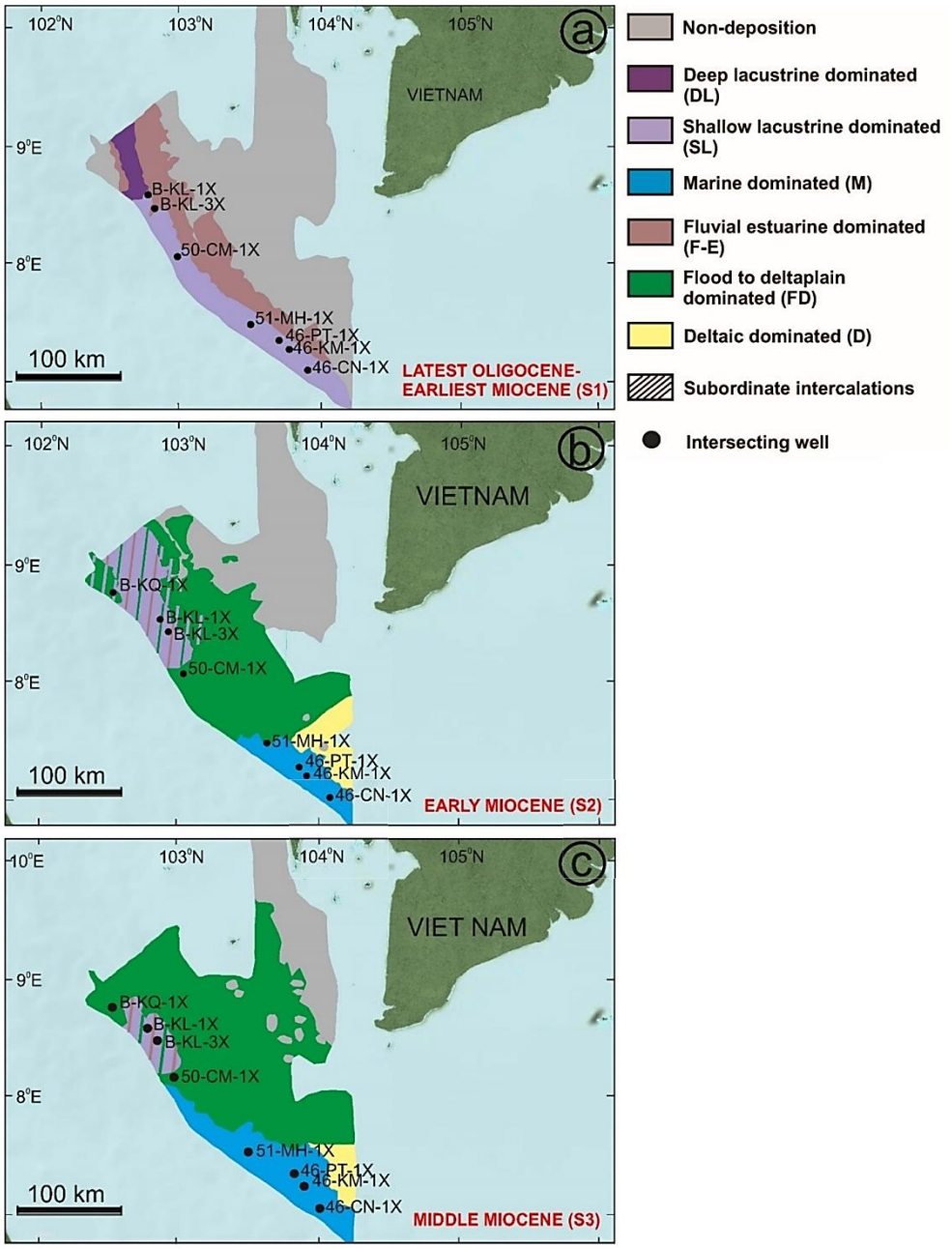

Figure 4. Uppermost Oligocene to Recent average gross depositional outline of Sequence S1 to S6 in the Malay-Tho Chu Basin

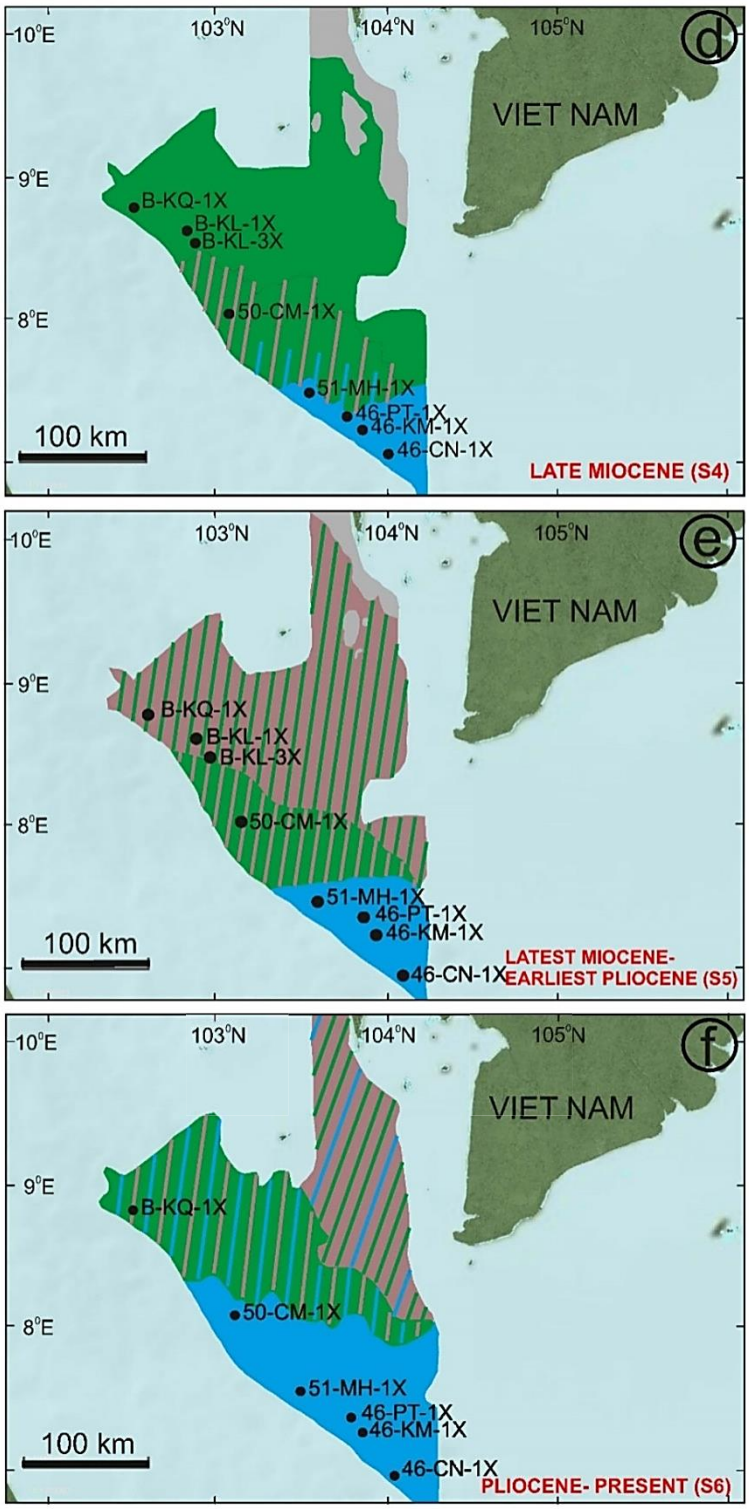

Figure 4. Cont.

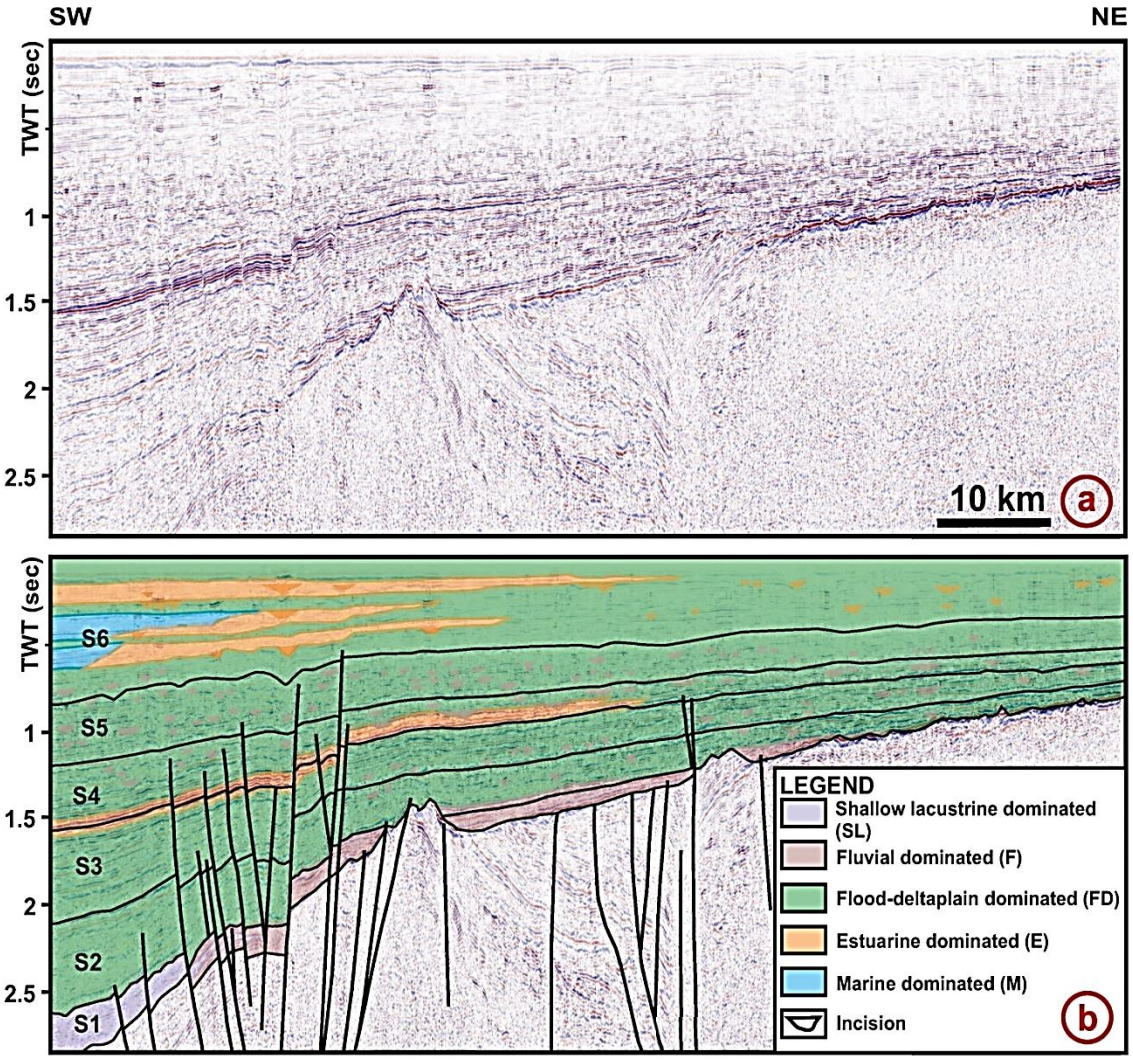

Figure 5. Uninterpreted northeast - southwest seismic section in the central Malay-Tho Chu Basin trending perpendicular to the regional dip (a) and its seismic facies interpretation (b). Cenozoic strata rest unconformably on a deformed section of Cretaceous through Paleozoic strata (Fyhn et al. 2010b). S1 is dominated by shallow lacustrine and fluvial depositits. S2 to S5 are dominated by the flood- and delta plain seismic facies association with fluvial filled channels. The fluvial channels are very abundant within S4 and especially S5. An increased marine influence is recorded within S6, although flood- and delta plain facies also seem to dominated the intersected succession. Location shown on Fig. 1

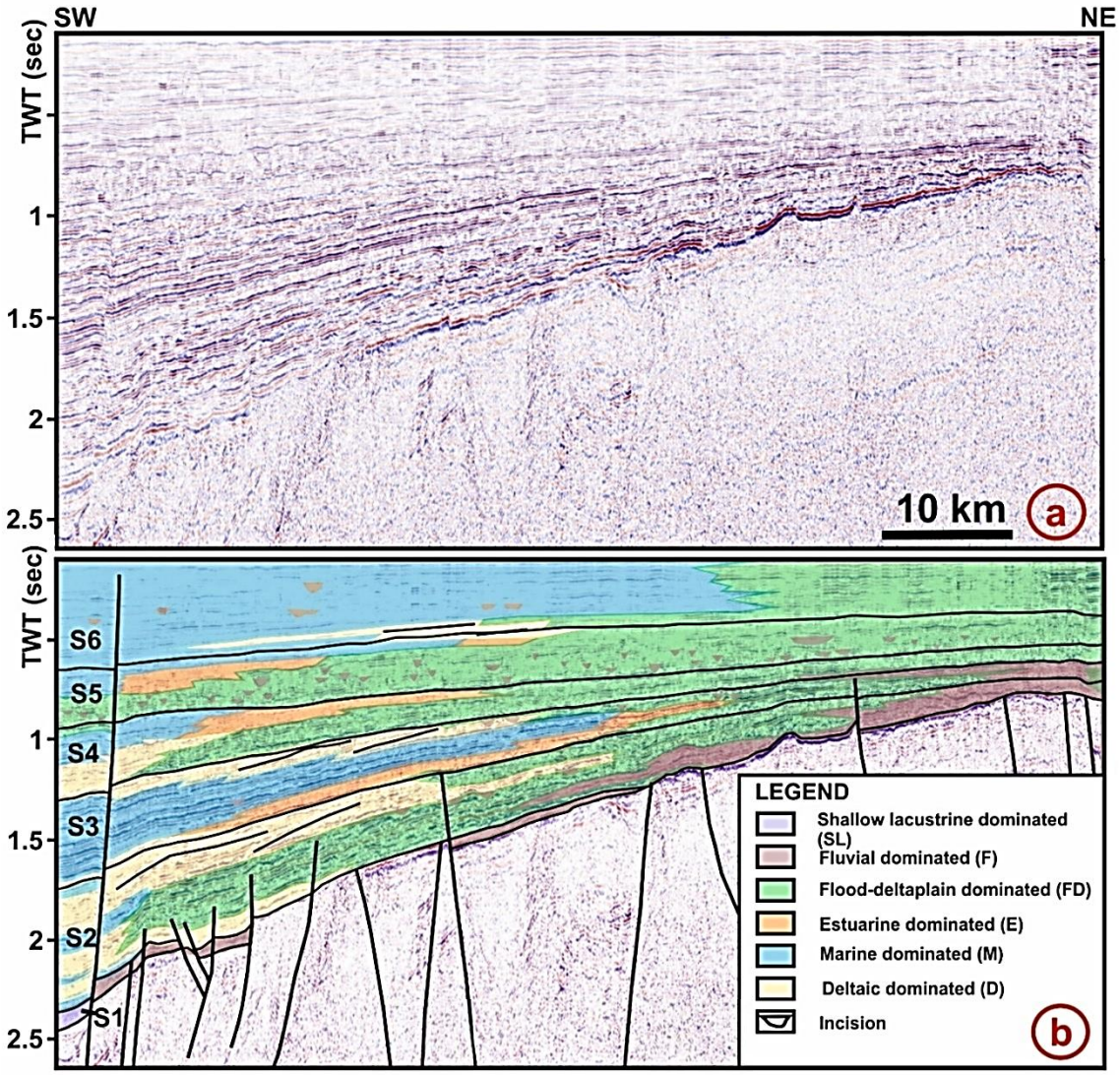

Figure 6. Uninterpreted northeast - southwest trending seismic section located perpendicular to regional dip in the southern Malay-Tho Chu basin (a) and its seismic facies interpretation (b). S1 is dominated by shallow lacustrine and fluvial facies associations. S2 to S6 are composed by the flood- and delta plain to shallow marine seismic facies associations. The marine influence increases upwards through S1 to S3. S4 and S5 records a decrease in marine influence with several fluvial incisions occuring in especially the upper part of the two sequences. The marine influence increases again from the upper part of S5 into S6 that is dominated by shallow marine deposits in the southwest. Location shown on Fig. 1

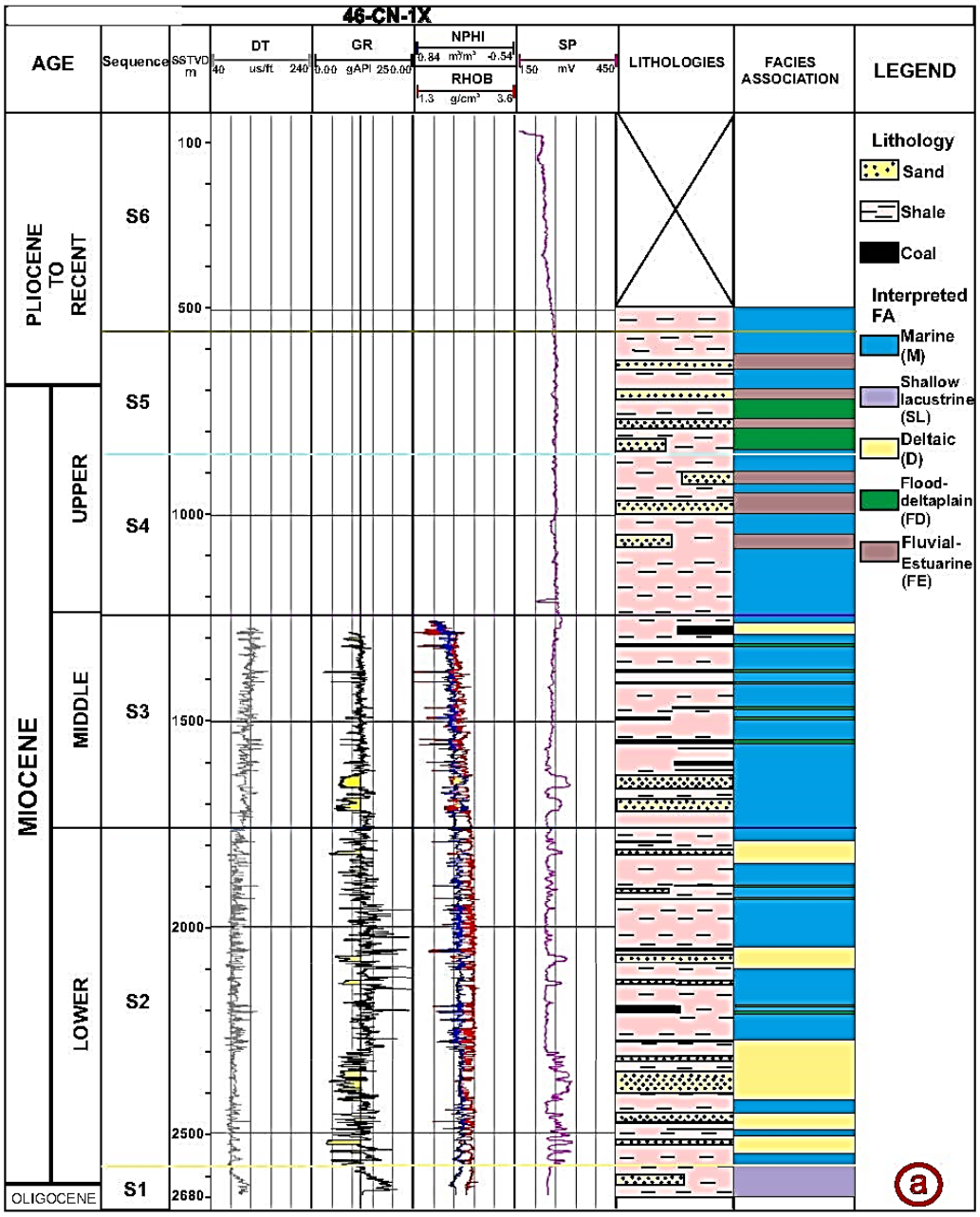

Figure 7. Well log and interpreted gross depositional facies (a) tied to uninterpreted northeast - southwest trending seismic section located perpendicular to regional dip in the southern Malay-Tho Chu basin (b) and its seismic facies interpretation (c). S1 is dominated by shallow lacustrine and fluvial deposits. S2 to S6 are composed by flood- and delta plain to shallow marine deposits. The marine influence increases upwards through S1 to S3. Apart from farthest south, S4 and S5 are non-marine dominated with several fluvial incisions occuring in especially the upper part of the two sequences. The marine influence increases again from the upper part of S5 into S6 that is dominated by shallow marine deposits in the southwest. Location shown on Fig. 1

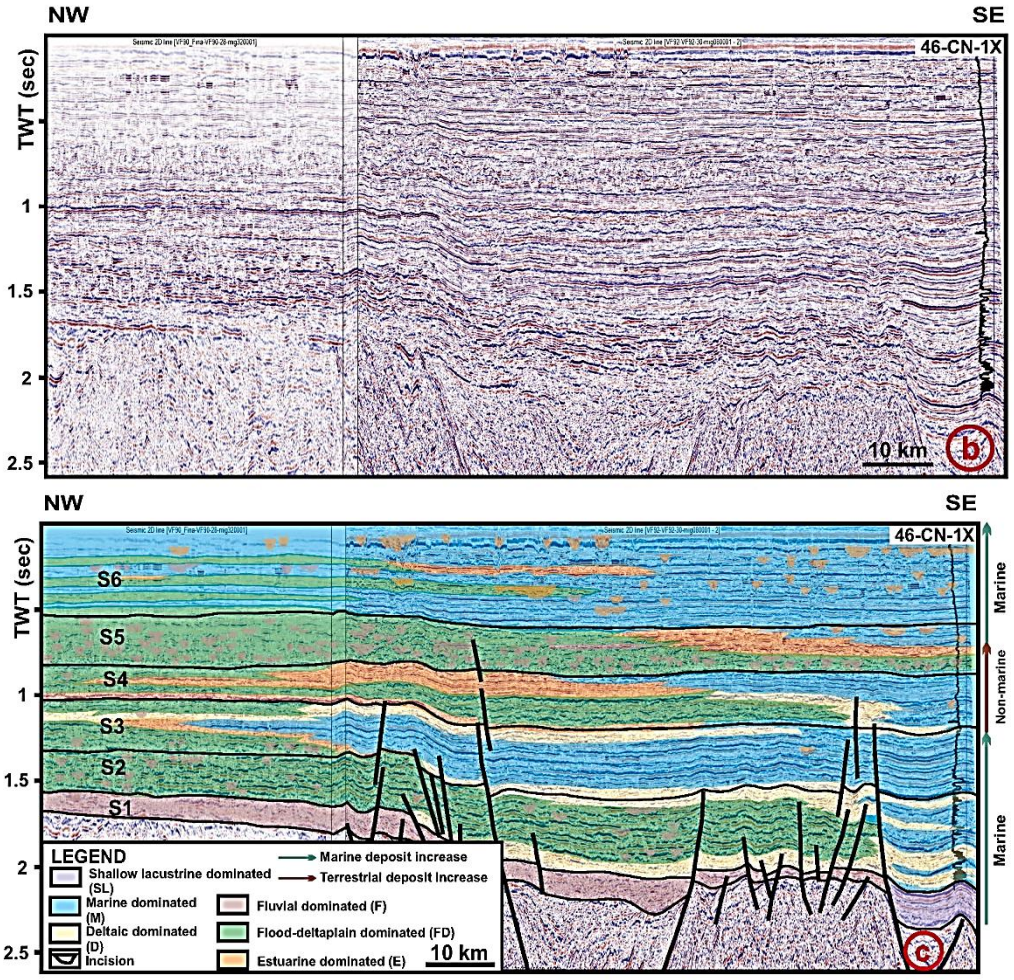

Figure 7. Cont.

4. Seismic facies associations

In the study area, six seismic facies associations have been determined: M, FD, D, SL, DL and F-E interpreted as marine-, flood- and delta-plain-, deltaic-, shallow lake-, deep lake- and fluvial-estuarine dominated, respectively, as argued below. They are described in the following sections in terms of their distributions, internal and external seismic reflection characteristics and their relation with adjacent seismic facies.

4.1. Facies association M (marine dominated)

4.1.1. Description

Seismic facies association M occurs in the depocenter in the southern part of the area. Parallel to sub-parallel, continuous reflectors distinguish facies association M from other facies associations (Fig. 8). Reflection amplitudes vary from low to strong and frequencies also vary considerably from low to high. HHere and there, subtle south-southwest-ward offlaps occur within the facies association. Facies association M is concordant to the underlying strata and frequently intercalates with facies associations FD and D and in a few instances also with F-E occurring as isolated trough fill. Facies association M grades into facies association FD and D to the north and east, respectively.

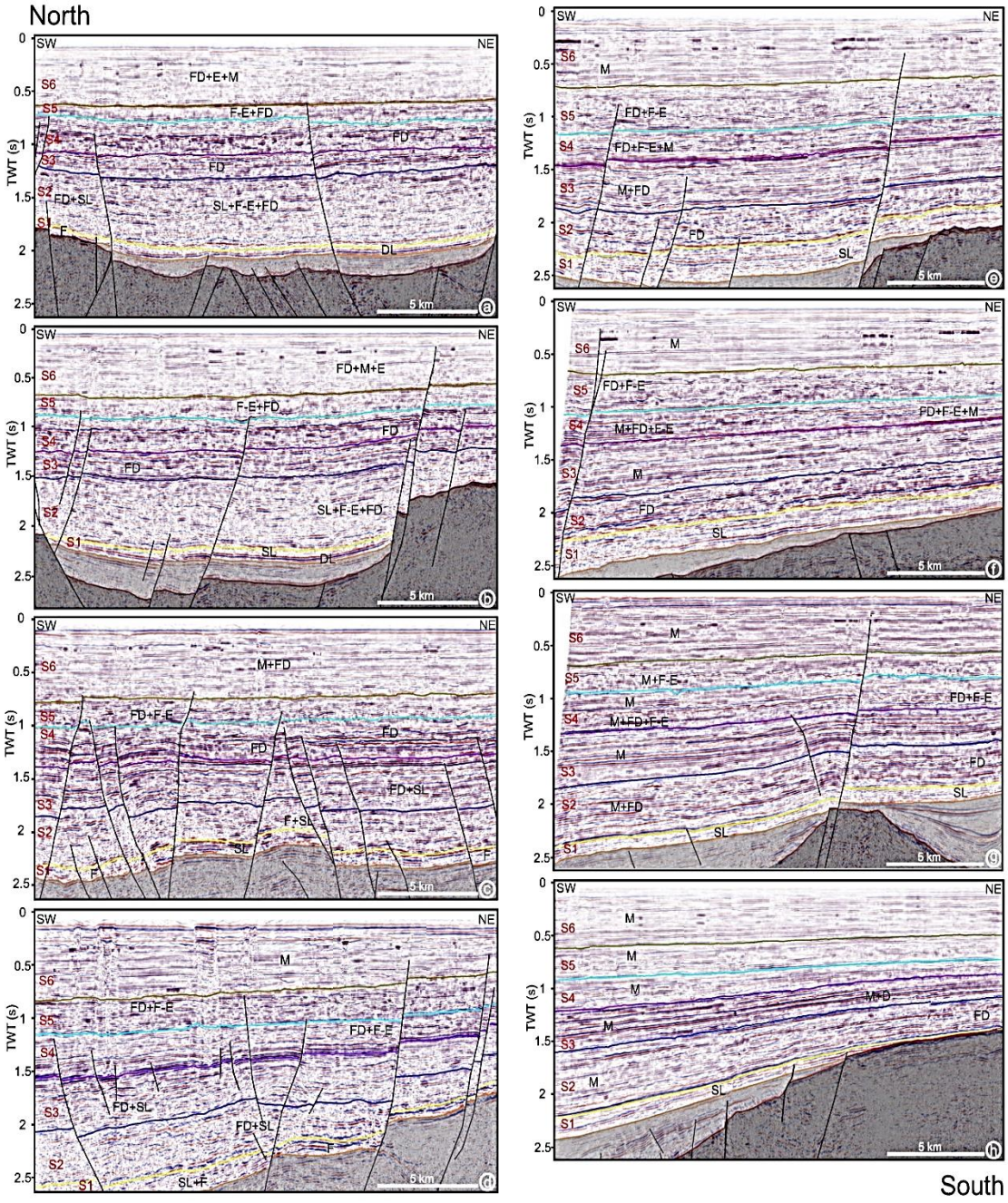

Figure 8. Seismic sections located over the southwestern MLTCB oriented parallel to each other. The sections are arranged in a north to south trending order to illustrate the lateral variation in seismic facies across the basin including the overall southeastwards increase in marine conditions

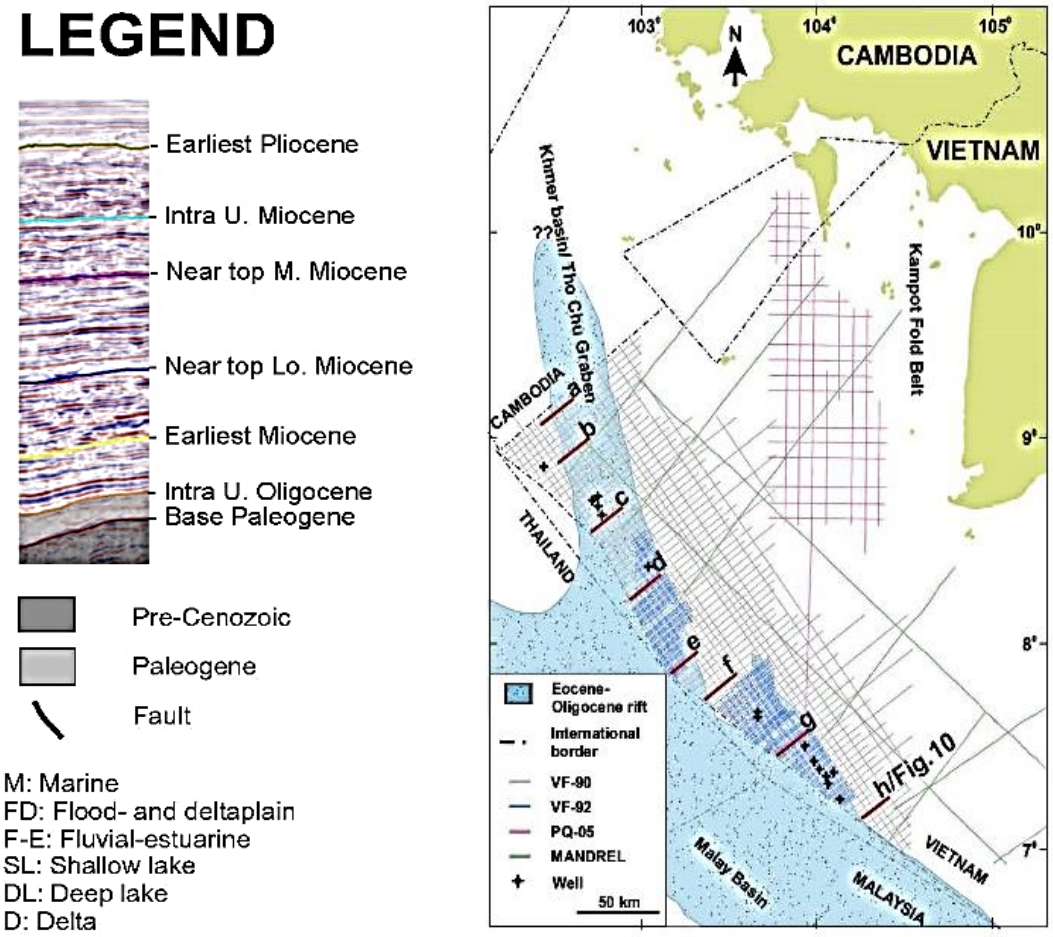

Figure 8. Cont.

4.1.2. Well information

Ditch cuttings retrieved from wells drilled into intervals dominated by facies M predominantly consist of claystones interbedded with sandstones and occasionally contains coal (Glover, 1997a, b; Glover and Phong, 1999a, b, c) (Fig. 7a). The facies association contains a variable foraminifera and nannofossils assemblage, which made Glover (1997a, b) and Glover and Phong (1999a, b, c) suggest a marine/inner neritic to coastal depositional environment for the drilled intervals intersecting facies association M.

4.1.3. Interpretation

The parallel reflection pattern of facies association M suggests broadly distributed depositional units. This fits well with the biostratigraphic evidence for a mostly shallow marine to near-shore depositional environment and with the southern part of the area dominated by the facies association M being located in the depocenter close to the East Vietnam Sea. The variable reflectivity probably corresponds to muddy accumulations alternating with sandy deposits in variable proportions. The scattered offlaps are interpreted as marine offlaps suggesting more distal marine conditions to the south-southwest of the study area.

4.2. Facies association D (deltaic dominated)

4.2.1. Description

Seismic facies association D mostly developed along the margin of depocenters. The facies association is characterized by subtle, shingled clinoforms formed by sub-parallel to slightly diverging reflectors that occasionally offlap towards depocenters. Facies association D has intermediate to high frequencies, intermediate to high amplitudes and intermediate reflection continuities. It intercalates with facies associations M and SL that are best developed basinward from facies association D. Away from the basin center, facies association D intercalates with facies association FD. Moreover, channelized incisions belonging to facies association F-E occur within the facies.

4.2.2. Well information

The thickest and seismically best developed examples of facies association D remains undrilled. Meanwhile, locally developed intervals of facies association D up to tens of meters thick occur in wells. These intervals are characterized by mixed mudstones and up to tens of meters thick sandstones. These intervals contain palynomorph-dominated fossil associations, in addition to few foraminifers and calcareous nannoplankton, which together with the lithology was interpreted by Glover (1997) to indicate a near-shore depositional setting strongly affected by fluvial input.

4.2.3. Interpretation

The subtle shingled clinoforms of facies association D could indicate a deltaic depositional environment facing relatively shallow waters (few tens of meters deep). This fits with its marginal position to the marine (M) and the depositional interpretation offered by Glover (1997) based on lithology and biostratigraphy.

4.3. Facies association FD (flood- and delta plain dominated)

4.3.1. Description

Seismic facies association FD is widely developed outside the depocenter over the eastern and northeastern basin margin, but also occurs within the depocenter in the west. Facies FD is characterized by a hummocky and semi-continuous to discontinuous internal reflection pattern commonly including 10-20 ms TWT (Two-Way travel Time) thick channelized incisions belonging to facies association F-E described below.

Frequencies tend to vary from low to intermediate and amplitudes from intermediate to strong. Facies association FD tends to be conformable with underlying strata apart from in the northeast where it onlaps and buries the base Cenozoic unconformity. The facies association intercalates with, and laterally grades into, facies association M, D, SL and F-E.

4.3.2. Well information

Facies association FD is intersected by exploration wells located in the northwest (e.g. B-KQ-1X, 50-CM-1X, B-KL-1X, B-KL-3X). Ditch cuttings retrieved from well 50-CM-1X drilled into facies FD are dominated by claystone with a subordinate content of sand and siltstones occasionally interbedded with lignite (Glover and Phong, 1999c). The fossil assemblage of facies association FD is dominated by spores and pollens with no or scattered foraminifers and nannofossils recorded. The biostratigraphic analysis of the facies association in well 50-CM-1X complemented by the lithology was interpreted to indicate delta plain deposition (Glover and Phong, 1999c), which fits well

with the freshwater dominated depositional environment suggested by Hung and Cable (1997) and Vinh and Cable (1998) for FD-intervals drilled in the B-KQ-1X, B-KL-1X and B-KL-3X wells located farther north.

4.3.3. Interpretation

The hummocky and semi- to discontinuous reflection pattern suggests a laterally variable depositional environment. Together with the common channelized incisions (around 10 to 30 m deep) and the biostratigraphic record, this fits with a flood- and delta plain depositional environment. This is compatible with facies association FD being situated landward of the M and D facies associations and often being developed in proximal settings located next to areas of uplift and non-deposition.

4.4. Facies association SL (shallow lake dominated)

4.4.1. Description

Seismic facies association SL occurs both above Eocene-Oligocene rift depocenters and over structural highs in the southern and southwestern parts of the study area (Fig. 8). The facies association mostly forms tabular sheets either resting on the Eocene-Oligocene rift succession, on the pre-Cenozoic or occurring as tens to several tens of ms TWT thick sheets intercalated with facies association F-E described below within the uppermost Oligocene to Middle Miocene succession. The base of the facies association is mostly parallel to the underlying successions, but onlaps and wedging outs occur towards structural highs.

Facies SL is characterized by semi-continuous to continuous reflections with highly variable amplitudes ranging from weak to strong and by intermediate frequencies with occasional low-frequency stringers. In general, the internal reflection pattern of facies SL is parallel to sub-parallel, but wavy reflectors and tens of ms thick trough-like incisions occur where facies association SL intercalates with facies association F-E. Facies association SL laterally grades into facies associations DL, F-E, D and FD.

4.4.2. Well information

The SL facies association is intersected by several exploration wells in the study area (e.g. 50-CM-1X, 51-MH-1X, B-KL-1X and 46-CN-1X). Ditch cuttings retrieved from intersecting wells are dominated by shale occurring together with sandstones (Glover, 1997a, b, c, d; Glover and Phong, 1999a, b). Biostratigraphic investigations together with the lithology made Glover (1997a, b, c, d), Glover and Phong (1999a) and Vinh and Cable (1998) suggest that these sediments formed in lacustrine to coastal plain settings.

4.4.3. Interpretation

The lacustrine to coastal plain depositional environment interpreted from the biostratigraphic data (Glover, 1997a; b; c; d; Glover and Phong, 1999a; Vinh and Cable, 1998) fits with the seismic characteristics that resemble shallow to marginal lacustrine successions elsewhere along the Vietnamese margin (Fyhn et al., 2020). This is in line with facies SL being developed above grabens and continuing over adjacent highs and occasional containing marine influenced interludes as suggested by biostratigraphy.

4.5. Facies association DL (deep lake dominated)

4.5.1. Description

During the latest Oligocene to earliest Miocene, seismic facies association DL formed above an Eocene-Oligocene rift depocenter in the west. Deposition of facies

association DL occurred when deposition went from being confined to Eocene-Oligocene grabens and half-grabens to taking place over wider areas and being less controlled by faulting during the Neogene (Fyhn et al., 2010a), The facies is typically composed of low to very low frequency, high amplitude and highly continuous reflections. Reflectors are internally parallel and typically drape the underlying succession. The facies appears as lenticular bodies above rift depocenters (Fig. 8b). Along the graben or half-graben margins, the facies laterally grades into the SL facies association with less continuous reflections or it pinches out and onlaps bounding faults or the underlying sequence. The facies association upwards grades into the SL facies association.

4.5.2. Well information

Facies association DL has not been intersected by exploration wells available to the study. However, the B-KL-1X well intersected the same stratigraphic interval (S1) very close to the DL facies association, but in a more proximal position located along the flank of a faulted high. The well encountered a mudstone-dominated succession occasionally with Total Organic Contents (TOC) between 1 and 5% and hydrogen index' (HI) between 300 and 500 mgHC/gTOC. Together with the palynomorph assemblage contained within the succession, this made Vinh and Cable (1998) interpret a lacustrine depositional setting for this unit located next to the DL facies association.

4.5.3. Interpretation

The succession and successions with compatible seismic characteristics found in similar settings have previously been interpreted as deep lacustrine deposits in other parts of the Gulf of Thailand and along the Vietnamese margin (Leo, 1997; Fyhn et al., 2009; 2020; Burton and Wood, 2010; Petersen et al., 2011). A lacustrine origin is also supported by palynology and high TOC and HI from cuttings retrieved from the B-KL-1X well drilled along the flank of the facies association. The higher reflection continuity and amplitude of the DL facies association together with the setting located above the depocenter of an Eocene-Oligocene rift depression and the TOC and hydrogen index is compatible with a more distal, deep lacustrine depositional environment compared to the one drilled in the well. The high amplitude characterizing the facies association could result from the presence of thickly developed organic rich successions intercalated with organic lean succession (Fyhn et al., 2020), which is in line with the organic rich mudstones in the neighboring well.

4.6. Facies association F-E (fluvial-estuarine dominated)

4.6.1. Description

Seismic facies association F-E can be subdivided into two sub-facies based on the external shape and reflectivity: 1) laterally continues sheets and 2) infill of channelized incisions.

The sub-facies occurring as laterally continuous sheets onlap and fill in relief on the base-Cenozoic unconformity or caps the Eocene-Oligocene syn-rift. It is characterized by hummocky, semi- to discontinuous reflections with variable reflection amplitudes, but mostly includes strongly reflected intervals or high amplitude streaks. The sheet facies association is interbedded with the SL facies association and laterally grades into facies associations SL or FD or

occurs as isolated pods onlapping the base-Cenozoic or top of the Eocene-Oligocene syn-rift.

The channelized sub-facies is mainly characterized by its external shape composed by ~10-50 ms deep erosive troughs few hundred meters to few kilometers across (Fig. 9). The channelized incisions are typically erosively cut into facies association FD but also occur within SL, D and M. The channel fill onlaps the incised troughs and is composed by chaotic or wavy reflectors of highly variable amplitude. The channelized sub-facies is most abundant in more proximal settings to the north and northeast, but are more widespread, and also occur farthest to the southwest, within certain stratigraphic intervals.

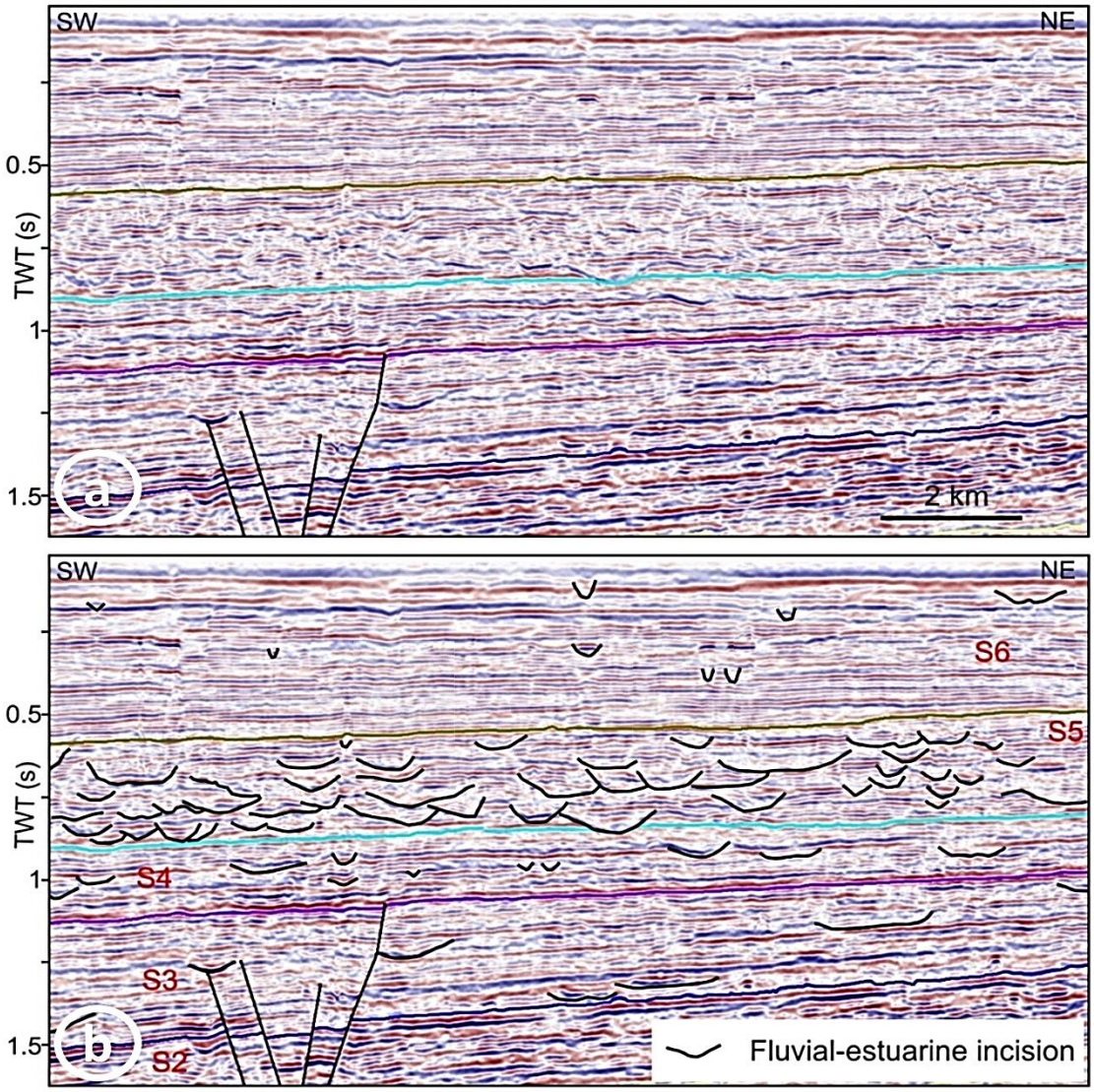

Figure 9. Seismic section illustrating stacked fluvial incisions within S5 filled with both fluvial estuarine deposits (a: uninterpreted, b: interpreted). Location shown on Fig. 1

4.6.2. Well information

Thick sections of the sheeted F-E facies association remain to be drilled. Thinner sections have been intersected in the B-KL-1X and B-KL-3X wells that was drilled near where facies association SL meets F-E. In these wells, sandy, fining upwards sections up to few tens of meters in thickness occur (Vinh and Cable, 1998; Cable and Vinh, 2000). They occur in intervals dominated entirely by palynomorphs that was interpreted to indicate a freshwater dominated depositional environment.

Successions including the channelized facies association F-E have been drilled in B-KL-1X, B-KQ-1X, 50-CM-1X, 46-NH-1X, 46-KM-1X, 46-CN-1X. The succession containing the facies association consists of sand- and mudstones interbedded with siltstones and traces of lignite. The sand content appears to be larger in the northwestern wells, whereas the wells to the southeast typically are more mudstone dominated. The intervals contain a fossil assemblage dominated by palynomorphs. In the wells farthest northwest, the fossil assemblage was interpreted to have formed in a freshwater dominated setting with scattered marine intervals (Hung and Cable, 1997; Vinh and Cable, 1998; Cable and Vinh, 2000). In the wells to the southeast, the fossil assemblage was interpreted to indicate a strong marine influence or even marine-dominated (Glover, 1997a; b; Glover and Phong, 1999a; c).

4.6.3. Interpretation

The sheets sub-facies association F-E are interpreted to represent fluvial-dominated strata based on its reflection characteristics that mimics fluvial deposits in other parts of the Vietnamese margin (Smith et al., 2019; Fyhn et al., 2020), and its isolated and proximal occurrence in relation to the other facies. In addition, the sandy, fining upwards sections encountered in the B-KL-1X and B-KL-4X wells may resemble the infill of fluvial channels. This also fits with the palynological indications of a freshwater dominated depositional environment (Vinh and Cable, 1998; Cable and Vinh, 2001).

The channelized sub-facies association F-E resembles fluvial incisions. This fits with the incisions occurring most commonly in proximal settings to the north and northeast and to a lesser extend farthest to the south.

The infill of the channels is probably composed both by fluvial and estuarine deposits. The sand dominated successions encountered in the wells farthest to the northwest interpreted to have formed primarily in freshwater environments are interpreted as overall fluvial dominated and only includes few marine-influenced interbeds. Meanwhile, the fossil assemblages in the mud-dominated succession corresponding to facies association F-E farther south were interpreted to be much more marine influenced (Glover, 1997a; b; Glover and Phong, 1999a; c). This is interpreted to indicate a greater content of estuarine infill of the incised channels in the southeast.

5. Sequences and the distribution of facies associations in each sequence

The latest Oligocene to Recent has been subdivided into six seismic sequences: S1, S2, S3, S4, S5 and S6. Each sequence is described below in terms of its base, age, thickness and the internal distribution of facies associations.

The depositional facies associations are mapped in each sequence and presented in Fig. 4.

5.1. Sequence 1, uppermost Oligocene to lowermost Miocene

Sequence 1 (S1) formed during the initial post-rift period above Eocene-Oligocene grabens and half-grabens along the southwestern part of the study area (Figs. 2, 4). Sequence 1 is dated as the latest Oligocene to earliest Miocene based on information from intersecting wells available in well completion reports (Cable and Hung, 2000; Glover, 1997a; Vinh and Cable, 1997). The base of S1 is marked by a strong reflection in most of the study area, and S1 rests conformably on the Paleogene rift sequence. Over structural highs and along graben margins, S1 rests directly on and onlaps pre-Cenozoic strata (Figs. 2, 5). In these areas, the base of S1 forms a prominent angular unconformity (Fig. 2). S1 is offset by normal faults initially established during the rift phase (Fyhn et al., 2010a), but few abrupt thickness variations of S1 occur over these faults (Fig. 5). The thickness of S1 is up to 250 ms TWT above grabens/half-grabens. The sequence pinches out shoreward and to the west and is absent farthest to the west and in the northeast.

Sequence 1 is composed by three seismic facies associations comprising the deep lacustrine dominated, the shallow lacustrine dominated and the fluvial dominated deposits associations (Fig. 4a).

The deep lacustrine dominated facies association developed in a depocenter over an Eocene-Oligocene rift depression in the west (Figs. 4, 8b). The deep lake facies association to the south grades into the shallow lacustrine dominated facies association distributed over grabens and half-grabens to the southwest, but occasionally continuing over structural highs as a thin veneer. The lacustrine facies associations grade into the fluvial dominated facies association developed over the flanks of former grabens and above structural highs (Fig. 4a). The fluvial facies association onlaps the base of the Sequence 1 causing the sequence to pinch out in a landward direction (Fig. 5).

5.2. Sequence 2, Lower Miocene

Sequence 2 (S2) is dated to be Early Miocene (Glover, 1997a; Glover and Phong, 1999a, b, c) corresponding to a very roughly six million years long period (~22-16 Ma). Sequence 2 rests conformably on S1 (Fig. 2) and is distributed over a larger area, extending east, northeast, and west of S1. Thus, S2 onlaps the pre-Cenozoic in the east and northeast of the study area as well as farthest to the west (Fig. 2, 4). The base of S2 is generally outlined by a strong amplitude reflector.

S2 is affected by growth faulting with fault offsets increasing towards the west (Figs. 2, 8). The thickest developed parts of S2 developed in down-faulted areas in the west. Here, S2 attains a thickness of approximately 650 ms TWT corresponding to approximately 1150 m using acoustic velocity information from nearby wells. The thickness of S2 and the duration of the depositional period suggest an average sedimentation rate of around 190 m/m.y. in the depocenters of S2 disregarding post-depositional compaction.

The infill of S2 is grouped into marine, flood- and delta plain, delta, shallow lacustrine and fluvial-estuarine facies associations. The marine facies association dominates the southern S2 (Figs. 4b, 8h). Towards the north, the marine facies association grades into the flood- and delta

plain facies association (Figs. 4b, 8e-g). Deltaic facies borders the marine facies association to the west.

The thickest part of S2 to the west is composed dominantly by the shallow lacustrine facies association interbedded with flood- and delta plain and fluvial-estuarine facies associations. These shallow lacustrine deposits of S2 cover the deep lacustrine deposits of S1. The shallow lacustrine dominated succession grades laterally into a seismic section primarily composed by the flood- and delta plain facies association away from the fault-controlled depocenter. Farthest south, S2 is mainly made from the marine seismic facies association characterized by continuous, parallel reflectors that grades into a deltaic dominated facies association to the northeast.

5.3. Sequence 3, Middle Miocene

Sequence 3 (S3) is dated to be Middle Miocene, corresponding to a roughly four million years long depositional period (~16-12 Ma) as indicated by the available biostratigraphic information (Glover and Phong, 1999a, b, c; Cable and Hung, 2000). S3 conformably overlies S2 but extends to the northeast of S2 where it onlaps the base-Cenozoic unconformity. Strata within S3 are generally parallel or subparallel with the base of the sequence, but onlaps the pre-Cenozoic towards the northeast. S3 is offset by normal faults, but the thickness of S3 is less affected by the faulting compared to the underlying thickness of S2.

The Middle Miocene comprises a sedimentary wedge with a thickness up to approximately 500 ms TWT in the depocenter above Paleogene grabens in the southwestern part of the study area. Towards the Vietnamese mainland, S3 fills in pre-existing topography within the base-Cenozoic surface, wedges out and is absent further to the northeast. Compared to S1 and S2, the thickness of S3 only varies moderately from over grabens to over adjacent structural highs.

The maximum thickness of roughly 500 ms TWT of S3 corresponds to approximately 675 m when comparing with the velocity information from wells intersecting S3. The thickness of S3 and the duration of the depositional period suggest an average depositional rate of around 170 m/m.y. in the S3 depocenter disregarding post-depositional compaction.

Sequence 3 consists of four main seismic facies associations comprising marine, flood- to delta plain, deltaic and fluvial-estuarine dominated deposits (Fig. 4c). A marine facies association dominates S3 farthest south (Figs. 4, 8f-h). Compared to S2, the marine facies association extends roughly 100 km farther to the northwest. The marine facies association to the north grades into a flood- and delta plain facies association. The flood- and delta plain facies association extends far north and west with the number of internal channelized incisions, belonging to the fluvial-estuarine facies association, increasing shoreward towards the northeast. In the west, the flood- and delta plain facies association intercalates locally with a succession dominated by shallow lacustrine and fluvial-estuarine facies associations as documented, especially, by well data (Fig. 4c) (Vinh and Cable, 1998; 2001). Farthest to the southeast, a deltaic facies association, characterized by prograding, shingled clinoforms intercalate with the marine facies association (Fig. 10).

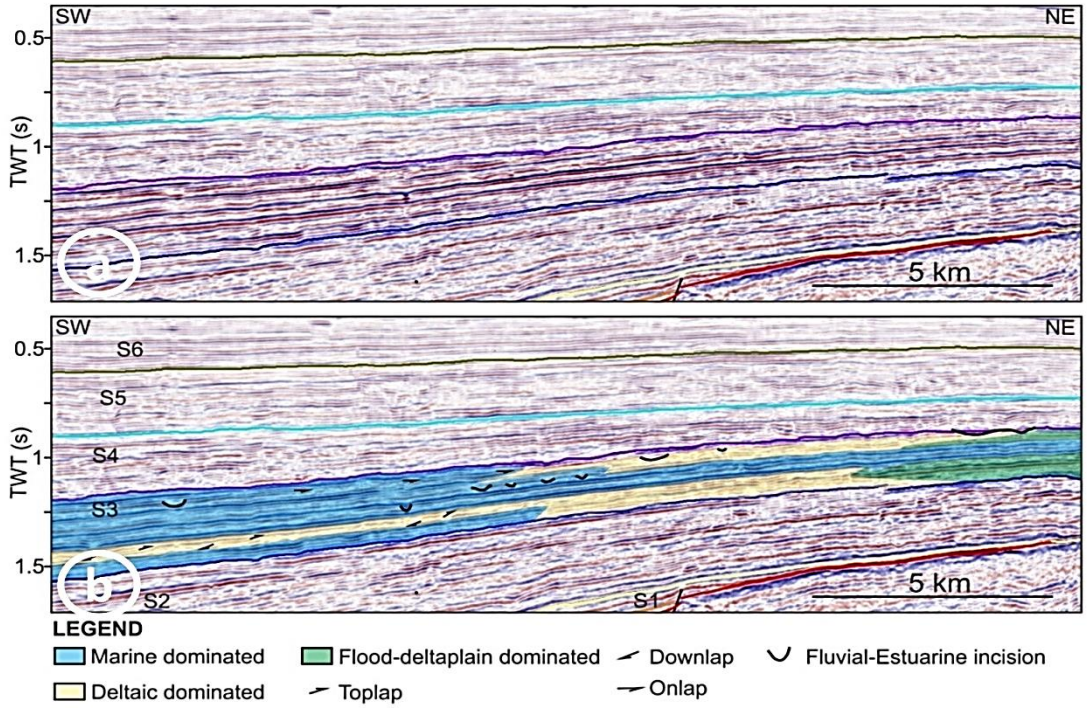

Figure 10. Seismic section (a: uninterpreted, b: interpreted) illustrating the intercalation of marine, deltaic and flood- to delta plain seismic facies associations within Sequence 3. Location shown on Fig. 1

5.4. Sequence 4, Upper Miocene

Sequence 4 (S4) formed during the Late Miocene over approximately five million years as indicated by the available biostratigraphic information (~12-7 Ma) (Glover, 1997a; Hung and Cable, 1997; Cable and Hung, 2000). The base of S4 in large areas is outlined by a strong, fairly continuous reflection grading into an intermediate to weak, less continuous reflection over structural highs (Fig. 5).

S4 is affected by growth faulting with moderate fault throws of less than 150 ms TWT (Fig. 2). The sequence attains a thickness of roughly 400 ms TWT in the depocenter to the southwest. The sequence wedges out to the northeast and is absent in the most landward part of the study area. S4 oversteps the distribution of S3 and therefore occurs farther landwards where it onlaps pre-Cenozoic strata filling in pre-existing topography.

The seismic thickness of S4 of up to 400 ms TWT corresponds to a thickness of approximately 450 m when converted using the velocity information available from intersecting wells. The thickness of S4 and the duration of the depositional period suggest an average sedimentation rate of up to roughly 90 m/m.y. disregarding post-depositional compaction.

Flood- to delta plain and marine dominated seismic facies associations prevail within S4, but the fluvial and estuarine facies association also makes up an important constituent, intercalating with the other two (Figs. 4d, 7). The flood- and delta plain facies association, with its hummocky, semi-continuous reflection pattern, makes up the northern and northeastern, landward parts of S4 outside the main depocenter (Fig. 4d). The flood- and

delta plain facies association within S4 contains numerous incised channels that are from few hundred meters to few kilometers wide belonging to the fluvial-estuarine facies association (Fig. 5). The channel abundance increases towards the south where the features form a stacked pattern intercalating with the flood- and delta plain facies association. Even farther south, the channelized fluvial-estuarine facies association decreases where the flood- and delta plain facies association intercalates with a marine facies association characterized by a fairly continuous and internally parallel reflection pattern.

The marine dominated facies association is distributed in the southernmost part of the area, close to the East Vietnam Sea. Towards the north, channel-shaped incisions of the fluvial-estuarine facies association occur within the marine dominated facies association. Moreover, gently inclined clinoforms, belonging to the delta facies association, also occur in the north at the transition towards the flood- and delta plain facies association. The presence of nannofossils and the nature of the palynomorph assemblage suggest the channelized incisions are filled with estuarine strata (Glover and Phong, 1999).

5.5. Sequence 5, uppermost Miocene-lowermost Pliocene

Sequence 5 (S5) formed during the latest Miocene to Early Pliocene time over a depositional period probably extending roughly three million years (~7-4 Ma). The basal boundary of S5 is characterized by moderate amplitude, semi-continuous reflections conformable with the underlying sequence. Farthest to the north and northeast, S5 oversteps the older Neogene sequences and onlaps the top of the pre-Cenozoic. In this area, S5 fills in pre-existing topography.

Sequence 5 is roughly 300 ms TWT thick in the depocenter located in the southwest and is slightly affected by faulting (Fig. 2). The unit wedges out towards the northeast and is absent in the shoreward part of the study area. The maximum seismic thickness of ~300 ms TWT of S5 corresponds to approximately 350 m judging by the seismic-to-depth conversion in wells intersecting S5 (Glover, 1997 a, c; Glover and Phong, 1999c). The thickness of S5 and the duration of the depositional period suggest an average depositional rate of around 120 m/m.y. disregarding post-depositional compaction.

A fluvial-estuarine seismic facies characterized by countless stacked incised channels makes up the northern and northeastern part of S5 (Fig. 9). The facies intercalates with thinner intervals attributed to the flood- and delta plain facies association (Fig. 4e). Farther south, the flood- and delta plain facies association makes up most of the sequence, even though fluvial-estuarine channels remain abundant. Farthest to the south, the succession grades into a marine facies association making up most of S5 (Fig. 4e).

5.6. Sequence 6, Pliocene-Recent

Sequence 6 (S6) comprises sediments dated as Pliocene and younger in wells intersecting the interval (Hung and Cable, 1997; Glover and Phong, 1999c) (Fig. 2). Sequence 6, thus, probably formed during the most recent four million years (~4-0 Ma).

The base of the sequence is generally outlined by an intermediate to strong reflection with moderate to high continuity over the depocenter in the west and southwest but losing continuity and amplitude landward. Farthest to the north, the base of S6 corresponds to the top of pre-Cenozoic marked by a pronounced erosional unconformity. S6 in this area fills in pre-existing topography.

Sequence 6 is slightly affected by faulting (Fig. 2). It is up to 600 ms TWT thick in the

depocenter in the west and southwest, but shoreward gradually wedges out and is around 100 ms TWT thick farthest landward. The 600 ms TWT seismic thickness of S6 corresponds to approximately 500 m in drilled sections. The thickness of S6 and the duration of the depositional period suggest an average depositional rate of roughly 125 m/m.y. in the depocenter disregarding post-depositional compaction.

The interpretation of the seismic facies pattern of S6 is challenged by multiples obscuring part of the primary signal. Even so, three main facies associations can be distinguished comprising the marine, the flood- and delta plain and the fluvial-estuarine facies associations. The distribution of the facies associations is shown in Fig. 4.

The marine facies association dominates most of the southern half of S6, thus representing a large expansion of the marine facies association compared with S5 (Fig. 4e, f). Northwards, the marine facies association intercalates with the flood- and delta plain facies association dominating the central part of the area. S6 in the central area also includes incised channels of the fluvial-estuarine facies association. To the north, channel incisions increase in abundance and the fluvial-estuarine facies association dominates over the flood- and delta plain facies association that they intercalate with. More continuous reflection stringers of the marine facies association intercalate with the other facies associations, even farthest north.

6. Discussions

6.1. Eustatic influence on deposition

The depositional record in the MLTCB contains a history of transgressions and regressions through time corresponding to changes in relative sea level. While the long-term latest Oligocene through Middle Miocene transgression recorded in the basin to some extent resembles eustatic sea level curves (Haq et al., 1987; Kominz et al., 1998; Betzler et al., 2018; Miller et al., 2020), the Late Miocene through Pleistocene pattern does not match the global eustatic sea level (Fig. 3). Much of the changes in relative sea level recorded in the basin must reflect a local governance of long-term relative sea level. This points towards a significant local control on relative sea level rooted in subsidence and infill rates governed by e.g. climate and tectonism.

On the other hand, the stacked channels with estuarine infill, especially well-developed within S4-S6, document rapid sea level fluctuations with a magnitude probably in the order of tens of meters judging by the depth of the incised channels. This is compatible with short-term Neogene glacio-eustatic variations (Miller et al., 2005; 2020) suggesting a strong impact of global relative sea-level changes on the shorter term deposition in the MLTCB.

Eustatic sea-level fluctuations, together with autocyclic processes, are likely to have affected older sequences also. This is most likely often the case when biostratigraphic information cited in well reports are used as indicators of marine influence in otherwise non-marine dominated intervals (and *vice versa*) reflecting the presence of marine interbeds. While the impact of short-term sea level fluctuations is associated with interbeds often below 2D seismic resolution that mostly images long-term trends.

The episodic marine inundation of the MLTCB during most of the Neogene documented here contrasts with Sarr et al. (2019) arguing that the widespread shallow seaways covering much of modern Sundaland only started to form during latest Pleistocene interglacials. Furthermore, a Pleistocene long-term subsidence rate of 200-300 m/Myr postulated for the entire Sunda shelf (Sarr et al., 2019) clearly far exceeds that observed in

the MLTCB. Hence, subsidence rates vary greatly across the Sundaland shelf, and likely only basin centers experienced long-term rates of 200-300 m/Myr during the Pleistocene.

6.2. Climatic and tectonic control on deposition

6.2.1. Impact of local and regional basin tectonics

Following the latest Oligocene-earliest Miocene, the change from deep/shallow lacustrine deposition to shallow lacustrine, fluvial and flood- and delta plain dominated sedimentation reflects the filling of rift-related topography associated with the decrease in rift-controlled subsidence. Instead, more regional subsidence commenced resulting in burial of formerly elevated areas outside grabens (Fyhn et al., 2010a). Meanwhile, Early Miocene faulting added to the subsidence rates in the west, and thus promoted periods of shallow lacustrine deposition in the depocenter. Farther east, Early Miocene faulting was insignificant and flood- and delta plain deposition prevailed instead.

During the latest Oligocene to earliest Miocene, an initial marine influence is recorded by estuarine interbeds within S1. This change commenced during a shorter pulse of globally falling eustatic sea level [Miller et al., 2020] (Fig. 3), but simultaneously with the onset of seafloor spreading in the southwestern East Vietnam Sea starting 23.6 Ma sensu Li et al. (2014).

The marine influence in the MLTCB increased until near the end of the Middle Miocene. A similar transgression culminating during the Middle Miocene took place in the western Gulf of Thailand (Phoosongsee et al., 2019) suggesting that increasingly marine conditions affected a large part of the gulf. Even though eustatic sea level rose between the later Early Miocene and the earliest Middle Miocene, the Middle Miocene maximum transgression in the MLTCB occurred at a time with falling eustatic sea level. This suggests a strong local tectonic control of the Middle Miocene relative sea level in the Gulf of Thailand. By Middle Miocene time, the SW East Vietnam Sea had fully opened (Briais et al., 1993; Li et al., 2014) placing the Gulf of Thailand next to an ocean basin. While the subsidence-to-sediment input ratio controlled relative sea/lake level in the gulf, the increasingly marine conditions was promoted by the introduced vicinity to the East Vietnam Sea. Throughout the Early and Middle Miocene, basins and structural highs located in the west of the East Vietnam Sea subsided rapidly and were transgressed (Dung et al., 2018). This affected deposition in basins along the western East Vietnam Sea (Matthews et al., 1997; Fyhn et al., 2009; 2013; 2020; Dung et al., 2018) and most likely paved the way for a transgression of the Gulf of Thailand.

During the latest Middle to latest Miocene time, non-marine deposition broadened again, and fluvial incisions are very common within much of S4. The overall regression and retraction of marine conditions coincide with a reduction by nearly half of long-term depositional rates from ~170-190 m/m.y. to ~90 m/m.y. (Fig. 3). Together with the shift towards more proximal deposition, this suggests a decrease in the creation of accommodation space.

The decrease in the creation of accommodation space coincided with uplift and non-deposition in the Nam Con Son and Cuu Long basins and adjacent areas (Matthews et al., 1997; Dung et al., 2018; Morley et al., 2019). Contemporaneously in

part of the neighboring Malay Basin, a thick coal seam developed reflecting a pronounced slow-down of deposition and stagnation of subsidence (Robert Morley, pers.com., 2019). During the same period, inversion and uplift affected other parts of the Malay and most of the West Natuna basins (Olson and Dorobek, 2000; Morley, 2012). The depositional outline of the MLTCB does not indicate a significant influx of sediments derived from the inverted and uplifted part of the Gulf of Thailand located to the south. This suggest that the Gulf of Thailand basin inversion had little direct impact on concomitant basin formation in the MLTCB. The latest Middle to Late Miocene slow-down in subsidence was more likely a regional effect of the Middle to Late Miocene uplift in the southwestern East Vietnam Sea realm. The long-term early Middle to mid Late Miocene lowering of eustatic sea-level (Miller et al., 2005; 2020) partly overlapped with the event in the MLTCB and may have amplified the depositional response of the slow-down in creation of accommodation space. In addition to the slow-down of subsidence in the MLTCB, the temporary halt in subsidence in neighboring basins likely funneled drainage through the MLTCB boosting sediment input. Together with the coeval slowed subsidence, this led to the observed regression and retraction of marine conditions.

Subsidence- and accumulation rates likely increased during the latest Miocene (Fig. 3) but data are inconclusive due to the limitation of age resolution of S5. Even so, the latest Miocene coincides with renewed rapid subsidence in the southwestern East Vietnam Sea similar to in the Cuu Long and the Nam Con Son basins, thus supporting a causal link between the Middle and Late Miocene subsidence pattern in the MLTCB and the coeval Middle Miocene uplift and subsequent sagging in the southwestern East Vietnam Sea region (Morley, 2019; Dung et al., 2018; Clift & Wilsoon, 2023).

6.2.2. Hinterland development, climate and deposition

Tectonics and climate affect the outline and size of hinterlands as well as the weathering rates (Jones and Frostick, 2002). This has significant bearings on the sediment input and deposition in basins (Goodbred and Kuehl, 2000; Jones and Frostick, 2002; Clift et al., 2008). In Asia, Clift (2006) linked monsoon strengthening with increased erosion during the Early to Middle Miocene. In the southern Gulf of Thailand, the most humid Cenozoic period characterized by ever-wet climate took place during the Early to Middle Miocene following monsoon strengthening (Morley, 2012). Around the same time, denudation rates increased to the north of the MLTCB as suggested by apatite fission track analysis (Fyhn et al., 2016; 2023). These observations suggest that the Early to Middle Miocene monsoon strengthening resulted in increased precipitation and erosion in the MLTCB hinterland, probably exerting a significant control on the rapid Early and Middle Miocene clastic accumulation rates in the MLTCB.

The link between hinterland weathering and deposition in the MLTCB mimics the effects of the Early to Middle Miocene monsoon strengthening and its relationship with deposition elsewhere in Asia (Clift et al., 2014). For instance, increased Early Miocene depositional rates in the East Vietnam Sea and strong chemical weathering in the hinterland are attributed to strengthening of the East Asian monsoon system (Clift et al., 2004; Clift and Sun, 2006; Wei et al., 2006). Similarly, enhanced Early Miocene weathering in the Himalayas is accredited to strengthening of the South Asian summer monsoon system (Clift et al., 2008).

Latest Middle to early Late Miocene monsoon weakening roughly coincide with a decrease in depositional rates in the MLTCB, although the change towards more proximal deposition does not favor climate and hinterland processes as the main driver of this change. The subsequent latest Miocene probable increase in accumulation rates in the MLTCB coincided with a period of relatively week monsoonal strength and cooling (Clift et al., 2008; Morley, 2012). The simultaneous regression recorded within S5 in the MLTCB, co-occurring with a rise in eustatic sea level (Fig. 3), may suggest a driving mechanism resulting from increased sediment supply to the MLTCB. Increased Late Neogene sedimentation rates in the neighboring Cuu Long and Nam Con Son basins where attributed to increased input from the Mekong River. While Breitfeld et al. (2022) interpreted a 15-17 Ma establishment of modern Mekong River, Liu et al. (2017) suggested the onset of the modern Mekong River Delta around 8 Ma following avulsion from the northern Gulf of Thailand. Li et al. (2013) and Clift and Wilson (2023) noted a significant increase in sediment accumulation in and in front of the Mekong Delta from the Late Miocene and linked it with either establishment of modern Mekong River or enhanced onshore erosion caused by seasonal rainfall and catchment uplift. Following the same line of thoughts, Miao et al. (2017) noted a latest Miocene increase in terrestrial fungal spores in East Vietnam Sea deep-marine sediments derived from the Mekong River and attributed the increase to an expansion of the Mekong River hinterland towards its present dimension. Bordering the modern Mekong Delta, the simultaneous increase in depositional rates in the MLTCB is likely also rooted in increased input from the river. Whether this Late Miocene increase reflects the onset of modern Mekong River, hinterland uplift, hinterland expansion or enhanced chemical weathering and erosion remains to be discerned.

During the Pliocene to Recent, accumulation rates in the MLTCB remained high. A similar pattern exists along the entire Indochina margin and in the central East Vietnam Sea recorded in dramatically increased subsidence and deposition in the Song Hong, Qiongdongnan, Phu Khanh and the Nam Con Son basins as well as in the central East Vietnam Sea (Matthews et al., 1997; Clift and Sun, 2006; Fyhn et al., 2009; 2013; Cao et al., 2017; Clift & Wilson, 2023). The increased depositional rates in these basins are attributed to enhanced SE Asian weathering resulting from regional hinterland uplift and Pliocene to Holocene monsoon strengthening (Carter et al., 2000; Molnar, 2004; Clift and Sun, 2004; Fyhn et al., 2023). Terrigenous supplies to the Gulf of Thailand and the MLTCB are also likely to have increased due to similar mechanisms rooted in climate and hinterland changes.

7. Conclusions

The uppermost Oligocene to Recent succession in the MLTCB is subdivided into six seismic sequences with variable seismic facies interpreted to reflect shallow marine, flood- and delta plain, fluvial-estuarine, deltaic and lacustrine sediments generally formed near sea level. This made depositional environments exposed to even small changes in tectonism, paleoclimate and eustatic sea level. While eustatic sea-level fluctuations induced short-lived transgressions and regressions during which channelized incisions formed in especially flood- and delta plain and marine dominated successions, tectonism and regional climate exerted the primary long-term control on deposition in the northeastern Gulf of Thailand. This suggests that tectonism and climate may outclass the signal of eustatic sea-level variation even in shallow shelf basins like the MLTCB.

From the latest Oligocene to the Middle Miocene, rapid subsidence and opening of the East Vietnam Sea, located next to the Gulf of Thailand, led to a transgression in the MLTCB. In the southern part of the area, this resulted in a change from lacustrine-fluvial dominated deposition in the latest Oligocene/earliest Miocene to marine dominated deposition. Farther north and west, flood- and delta plain deposition prevailed, although shallow lacustrine deposition continued for a while farthest west, driven by fast fault-enhanced subsidence. The Early and Middle Miocene depositional rates were high (up to 170-190 m/m.y.). This most likely resulted from hinterland uplift and rapid weathering forced by a hot and humid climate.

During the latter part of the Middle Miocene, a regression affected the MLTCB. The regression occurred during a period of slowed subsidence interpreted as linked with regional uplift in the southwestern East Vietnam Sea and neighboring basins. The regression resulted in a southward retreat of the shoreline and an expansion of flood- and delta plain deposition. The decrease in subsidence rate made the MLTCB vulnerable to eustatic sea-level fluctuations during this period, which resulted in the formation of incised channels filled with fluvial and estuarine strata. The regression culminated during the latest Miocene.

From the latest Miocene, subsidence rates increased, and the marine influence broadened from the south. Even so, fluvial-estuarine deposition prevailed in the north and flood- and delta plain deposition dominated in the central part of the MLTCB due to Mekong River avulsion to its present location increasing sediment input. Terrigenous depositional rates have remained high since then similarly to elsewhere offshore Indochina. The regional high rates probably reflect onshore regional uplift and enhanced erosion promoted by monsoon strengthening.

Acknowledgements

We would like to thank the Schlumberger Faculty for the Future Foundation for funding a Ph.D. grant to Tu Anh Nguyen from which this work springs. Schlumberger is also acknowledged for a university grant to the University of Copenhagen for Petrel and Vietnam Petroleum Institute and Petro Vietnam for the permission to access the dataset. The university of Copenhagen is thanked for housing Tu Anh Nguyen during her Ph.D.

References

Barckhausen U., Engels M., Franke D., Ladage S., Pubellier M., 2014. Evolution of the South China Sea (East Sea): Revised ages for breakup and seafloor spreading. Marine and Petroleum Geology, 58(PB), 599–611. https://doi.org/10.1016/j.marpetgeo.2014.02.022.

Barckhausen U., Roeser H.A., 2004. Seafloor spreading anomalies in the South China Sea (East Sea) revisited. Geophysical Monograph Series, 149 (July), 121–125. https://doi.org/10.1029/149GM07.

Betzler C., Eberli G.P., Lüdmann T., Reolid J., Kroon D., Reijmer J.J.G., Swart P.K., Wright J., Young J.R., Alvarez-Zarikian C., Alonso-García M., Bialik O.M., Blättler C.L., Guo J.A., Haffen S., Horozal S., Inoue M., Lovane L., Lanci L., Layla J.C., Hui Mee A.L., Nakakuni M., Nath B.N., Niino K., Petruny L.M., Pratiwi S.D., Slagle A.L., Sloss C.R., Su X., Yao Z., 2018. Refinement of Miocene sea level and monsoon events from the sedimentary archive of the Maldives (Indian Ocean). Progress in Earth and Planetary Science, 5, 18p. https://doi.org/10.1186/s40645-018-0165-x.

Breitfeld H.T., Hennig-Breitfeld J., BouDagher-Fadel M., Schmidt W.J., Meyer K., Reinprecht J., Lukie T., Cuong T.X., Hall R., Kollert N., Gough A., Ismail R., 2022. Provenance of Oligocene–Miocene sedimentary rocks in the Cuu Long and Nam Con Son basins, Vietnam and early history of the Mekong River. International Journal of Earth Sciences, 111, 1773-1804. https://doi.org/10.1007/s00531-022-02214-0.

Briais A., Patriat P., Tapponnier P., 1993. Updated interpretation of magnetic anomalies and seafloor spreading stages in the South China Sea (East Sea): implications for the Tertiary tectonics of Southeast Asia. Journal of Geophysical Research, 98B, 6299–6328.

Browning J.V., Miller K.G., McLaughlin P.P., Kominz M.A., Sugarman P.J., Monteverde D., Feigenson M.D., Hernández J.C., 2009. Quantification of the effects of eustasy, subsidence, and sediment supply on Miocene sequences, mid-Atlantic margin of the United States. GSA Bulletin, 118, 567–588.

Burton D., Wood L., 2010. Seismic geomorphology and tectonostratigraphic fill of half grabens, West Natuna Basin, Indonesia. AAPG Bulletin, 94, 1695–1712.

Cable G., Hung L.V., 2000. B-KL-3X, geological completion report, block B, offshore Vietnam. Unocal Vietnam Exploration Ltd., HCMC, Vietnam.

Cable G., Vinh L.N., 2000. B-KL-2X "Golden Dragon - Kim Long", geological completion report, block B, offshore Vietnam. Unocal Vietnam Exploration, Ltd., HCMC, Vietnam.

Cao Y., Li C-F., Yao Y., 2017. Thermal subsidence and sedimentary processes in the South China Sea (East Sea) Basin. Marine Geology, 394, 30–38.

Carter A., Roques D., Bristow C.S., 2000. Denudation history of onshore central Vietnam: Constraints on the Cenozoic evolution of the western margin of the South China Sea (East Sea). Tectonophysics, 322(3–4), 265–277. https://doi.org/10.1016/S0040-1951(00)00091-3.

Clift P.D., 2006. Controls on the erosion of Cenozoic Asia and the flux of clastic sediment to the ocean. Earth and Planetary Science Letters, 241(3–4), 571–580. https://doi.org/10.1016/j.epsl.2005.11.028.

Clift P.D., Hodges K.V., Heslop D., Hannigan R., Long H.V., Calves G., 2008. Correlation of Himalayan exhumation rates and Asian monsoon intensity. Nature Geoscience, 1, 875–880.

Clift P.D., Sun Z., 2006. The sedimentary and tectonic evolution of the Yinggehai-Song Hong basin and the southern Hainan margin, South China Sea (East Sea): Implications for Tibetan uplift and monsoon intensification. Journal of Geophysical Research: Solid Earth, 111(6), 1–28. https://doi.org/10.1029/2005JB004048.

Clift P.D., Wan S., Blusztajn J., 2014. Reconstructing chemical weathering, physical erosion and monsoon intensity since 25 Ma in the northern South China Sea (East Sea): A review of competing proxies. Earth-Science Reviews, 130, 86–102.

Clift P.D., Wilson L.J., 2023. Syn-and post-rift lower crustal flow under the Sunda Shelf, southern Vietnam: A role for climatically modulated erosion. Basin Research, 00, 1–30. https://doi.org/10.1111/bre.12809.

Dung B.V., Tuan H.A., Kieu N.V., Man H.Q., Huyen P.T.D., 2018. Depositional environment and reservoir quality of Miocene sediments in the central part of the Nam Con Son Basin, southern Vietnam shelf. Marine and Petroleum Geology, 97, 672–689.

Flower B.P., Kennett J.P., 1994. The middle Miocene climatic transition: East Antarctic ice sheet development, deep ocean circulation and global carbon cycling. Palaeogeography, Palaeoclimatology, Palaeoecology, 108(3–4), 537–555. https://doi.org/10.1016/0031-0182(94)90251-8.

Fyhn M.B.W., Boldreel L.O., Nielsen L.H., 2009. Geological development of the Central and South Vietnamese margin: Implications for the establishment of the South China Sea (East Sea), Indochinese escape tectonics and Cenozoic volcanism. Tectonophysics, 478(3–4), 184–214. https://doi.org/10.1016/j.tecto.2009.08.002.

Fyhn M.B.W., Boldreel L.O., Nielsen L.H., 2010a. Escape tectonism in the Gulf of Thailand: Paleogene left-lateral pull-apart rifting in the Vietnamese part of the Malay Basin. Tectonophysics, 483(3–4), 365–376. https://doi.org/10.1016/j.tecto.2009.11.004.

Fyhn M.B.W., Boldreel L.O., Nielsen L.H., Giang T.C., Nga L.H., Hong N.T.M., Nguyen N.D., Abatzis I., 2013. Carbonate platform growth and demise offshore Central Vietnam: Effects of Early Miocene transgression and subsequent onshore uplift. Journal of Asian Earth Sciences, 76, 152–168. https://doi.org/10.1016/j.jseaes.2013.02.023.

Fyhn M.B.W., Cuong T.D., Hoang B.H., Hovikoski J., Olivarius M., Tuan N.Q., Tung N.T., Huyen N.T., Cuong T.X., Nytoft H.P., Abatzis I., Nielsen L.H., 2018. Linking Paleogene rifting and inversion in the northern Song Hong and Beibuwan basins, Vietnam,

with left-lateral motion on the Ailao Shan - Red River Shear Zone. Tectonics, 37. https://doi.org/10.1029/2018TC005090.

Fyhn M.B.W., Green P., Hoang B.H., Hovikoski J., Tri T.V., Phach P.V., Thomsen T.B., Petersen H.I., Bojesen-Koefoed J.A., Abatzis I., Nielsen L.H., Heine C., 2023. Late Cretaceous and Cenozoic denudation of the northern Central Vietnam examined through apatite fission track analysis. Submitted to Journal of East Asian Earth Sciences.

Fyhn M.B.W., Green P.F., Bergman S.C., Van Itterbeeck J., Tri T.V., Dien P.T., Abatzis I., Thomsen T.B., Chea S., Pedersen S.A.S., Mai L.C., Tuan H.A., Nielsen L.H., 2016. Cenozoic deformation and exhumation of the Kampot Fold Belt and implications for south Indochina tectonics. Journal of Geophysical Research: Solid Earth, 121(7), 5278–5307. https://doi.org/10.1002/2016JB01284.

Fyhn M.B.W., Hoang B.H., Anh N.T., Hovikoski J., Cuong T.D., Dung B.V., Olivarius M., Tuan N.Q., Toan D.M., Tung N.T., Huyen N.T., Cuong T.X., Nytoft H.P., Abatzis I., Nielsen L.H., 2020. Eocene-Oligocene syn-rift deposition in the northern Gulf of Tonkin, Vietnam. Marine and Petroleum Geology, 111, 390–413. https://doi.org/10.1016/j.marpetgeo.2019.08.041.

Fyhn M.B.W., Pedersen S.A.S., Boldreel L.O., Nielsen L.H., Green P.F., Dien P.T., Huyen L.T., Frei D., 2010b. Palaeocene-early Eocene inversion of the Phuquoc-Kampot Som Basin: SE Asian deformation associated with the suturing of Luconia. Journal of the Geological Society, 167(2), 281–295. https://doi.org/10.1144/0016-76492009-039.

Fyhn M.B.W., Phach P.V., 2015. Late Neogene structural inversion around the northern Gulf of Tonkin, Vietnam: Effects from right-lateral displacement across the Red River fault zone. Tectonics, 34(2), 290–312. https://doi.org/10.1002/2014TC003674.

Ginger D.C., Pothecary J., Hedley R.J., 1994. New insights into the inversion history of the West Natuna Basin. AAPG Bulletin, 78(7), 1142–1143.

Glover S.P., 1997a. 46-CN-1X, final well geological report, block 46, offshore Vietnam. FINA Exploration Minh Hai B.V., HCMC, Vietnam.

Glover S.P., 1997b. 46-NH-1X, final well geological report, block 46, offshore Vietnam. FINA Exploration Minh Hai B.V., HCMC, Vietnam.

Glover S.P., 1997c. 46-PT-1X, final well geological report, block 46, offshore Vietnam. FINA Exploration Minh Hai B.V., HCMC, Vietnam.

Glover S.P., 1997d. 51-UM-1X, final well geological report, block 51, offshore Vietnam. FINA Exploration Minh Hai B.V., HCMC, Vietnam.

Glover S.P., Phong N.X., 1999a. 46-KM-1X, final well geological report, block 46, offshore Vietnam. FINA Exploration Minh Hai B.V., HCMC, Vietnam.

Glover S.P., Phong N.X., 1999b. 46-TL-1X, final well geological report, block 46, offshore Vietnam. FINA Exploration Minh Hai B.V., HCMC, Vietnam.

Glover S.P., Phong N.X., 1999c. 50-CM-1X/1X-ST, final well geological report, block 50, offshore Vietnam. FINA Exploration Minh Hai B.V., HCMC, Vietnam.

Goodbred S.L., Kuehl S.A., 2000. Enormous Ganges-Brahmaputra sediment discharge during strengthened early Holocene monsoon. Geology, 28, 1083–1086.

Gradstein F.M, Ogg J.G, Schmitz M.D, Ogg G.M., 2020. The geologic time scale 2020. Elsevier, Amsterdam, 2, 1357p.

Haq B.U., Hardenbol J., Vail P.R., 1987. Chronology of fluctuating sea levels since the Triassic (250 million years ago to present). Science, 235, 1156–1167.

Hoang B.H., Fyhn M.B.W. Hovikoski J., Boldreel L.O., Tuan N.Q., Dam M.H., Long H.V., Tung N.T., Nielsen L.H., Abatzis I., 2023. Cenozoic structural development of the western flank of the Song Hong Basin, Gulf of Tonkin, Vietnam: Linking with onshore strike-slip faulting and regional tectonics. Journal of Asian Earth Sciences, 246, 105581. https://doi.org/10.1016/j.jseaes.2023.105581.

Hoang B.H., Fyhn M.B.W., Cuong T.D., Tuan N.Q., Schmidt W.J., Boldreel L.O., Anh N.T.K., Huyen N.T., Cuong T.X., 2020. Paleogene structural development of the northern Song Hong Basin and adjacent areas: Implications for the role of extrusion tectonics in basin formation in the Gulf of Tonkin. Tectonophysics, 789, 228522. https://doi.org/10.1016/j.tecto.2020.228522.

Hung L.N., Cable G., 1997. B-KQ-1X, geological completion report, block B, offshore Vietnam. Unocal Vietnam Exploration Ltd., HCMC, Vietnam.

Hutchison C.S., 1996. Geological evolution of Southeast Asia. Geological Society of Malaysia, Kuala Lumpur, 368p.

Jaillard E., Yacobi L.A., Rebolet S., Robert E., Masrour M., Bouchaou L., Giraus F., Hariri K.E., 2019. Late Barremian eustacy and tectonism in the western High Atlas (Essaouira-Agadir Basin), Morocco. Cretaceous Research, 93, 225–244.

Jenyon M.K., Fitch A.A., 1985. Seismic Reflection Interpretation: Geoexploration Monographs, series 1 - No. 8, Geopublication Associates, Gebrüder Borntraeger, Berlin - Stuttgart, 318p.

Jones S.J., Frostick L.E. (Eds), 2002. Sediment Flux to Basins: Causes, Controls and Consequences. Geological Society, Special Publication, London, 191, 286p.

Kominz M.A., Miller K.G., Browning J.V., 1998) Long-term and short-term global Cenozoic sea-level estimates. Geology, 26(4), 311–314.

Lee G.H., Lee K., Watkins J.S., 2001. Geological evolution of the Cuu Long and Nam Con Son Basins, offshore southern Vietnam, South China Sea (East Sea). AAPG Bulletin, 85, 1055–1082.

Leo C.T.A.M., 1997. Exploration in the Gulf of Thailand in deltaic reservoirs, related to the Bongkot Field. In: Fraser A.J., Matthews S.J., Murphy R.W. (Eds.): Petroleum Geology of Southeast Asia, 126, 77–87.

Li C-F., Xu X., Lin J., Sun Z., Zhu J., Yao Y., Zhao X., Liu Q., Kulhanek D.K., Wang J., Song T., Zhao J., Qiu N., Guan Y., Zhou Z., Williams T., Bao R., Briais A., Brown E.A., Chen Y., Clift P.D., Colwell F.S., Dadd K.A., Ding W., Almeida I.H., Huang X-L., Hyun S., Jiang T., Koppers A.A.P., Li Q., Liu C., Liu Z., Nagai R.H., Peleo-Alampay A., Su X., Tejada M.L.G, Trinh H.S., Yeh Y-C., Zhang C., Zhang F., Zhang G-L., 2014. Ages and magnetic structures of the South China Sea (East Sea) constrained by deep tow magnetic surveys and IODP Expedition 349. Geochemistry, Geophysics, Geosystems, 15, 4958–4983. https://doi.org/10.1002/2014GC005567.

Li L., Clift P.D., Nguyen H.T., 2013. The sedimentary, magmatic and tectonic evolution of the Southwestern South China Sea (East Sea) revealed by seismic stratigraphic analysis. Marine Geophysical Research, 34, 393–406. Doi: 10.1007/s11001-013-9171-y.

Liu C., Clift P.D., Giosan L., Miao Y., Warny S., Wan S., 2019. Paleoclimatic evolution of the SW and NE South China Sea (East Sea) and its relationship with spectral reflectance data over various age scales. Palaeogeography, Palaeoclimatology, Palaeoecology, 525, 25–43. Doi: 10.1016/j.palaeo.2019.02.019.

Liu C., Clift P.D., Murray R.W., Blusztajn J., Ireland T., Wan S., Ding W., 2017. Geochemical Evidence for Initiation of the Modern Mekong Delta in the southwestern South China Sea (East Sea) after 8 Ma. Chemical Geology, 451, 38-54. Doi: 10.1016/j.chemgeo.2017.01.008.

Macdonald D.I.M (Ed.), 1991. Sedimentation, Tectonics and Eustasy: Sea-Level Changes at Active Margins. Willey, 518p. https://doi.org/10.1002/9781444303896.

Madon M., 2007. Overpressure development in rift basis: an example from the Malay Basin, offshore Peninsular Malaysia. Petroleum Geoscience, 13, 169-180.

Madon M.B.H., 1997. The kinematics of extension and inversion in the Malay Basin, offshore Peninsular Malaysia. GeoL. Soc. Maiaytlia, BuLletin, 41, 127–138. http://www.gsm.org.my/products/702001-100865-PDF.pdf.

Matthews S.J., Fraser A.J., Lowe S., Todd S.P., Peel F.J., 1997. Structure, stratigraphy and petroleum geology of the SE Nam Con Son Basin, offshore Vietnam. Geological Society, London, Special Publications, 126(1), 89–106. https://doi.org/10.1144/GSL.SP.1997.126.01.07.

Miao Y.F., Warnya S., Liua C., Clift P.D., Gregory M., 2017. Neogene fungal record from IODP Site U1433, South China Sea (East Sea): Implications for paleoenvironmental change and the onset of the Mekong River. Marine Geology, 394, 69–81.

Miller K.G., Browning J.V., Schmelz W.J, Kopp R.E., Mountain G.S., Wright J.D., 2020. Cenozoic sea-level and cryospheric evolution from deep-sea geochemical and continental margin records, Science Advances (in press).

Miller K.G., Kominz M.A., Browning J.V., Wright J.D., Mountain G.S., Katz M.E., Sugarman P.J., Cramer B.S., Christie-Blick N., Pekar S.F., 2005.

The phanerozoic record of global sea-level change. Science, 310(5752), 1293–1298. https://doi.org/10.1126/science.1116412.

Miller K.G., Mountain G.S., Wright J.D., Browning J.V., 2011. A 180-million-year record of sea level and ice volume variations from continental margin and deep-sea isotopic records. Oceanography, 24(2), 40–53. Doi: 10.5670/oceanog.2011.26.

Mitchum Jr. R.M., Vail P.R., Sangree J.B., 1977. Seismic stratigraphy and global changes of sea level, Part 6: Stratigraphic interpretations of seismic reflection patterns in depositional sequences. In: Payton, C.E. (Ed.), Seismic Stratigraphy Application to Hydrocarbon Exploration. AAPG Memoir, 26, 117–133. https://doi.org/10.1306/M26490C8.

Molnar P., 2004. Late Cenozoic increase in accumulation rates of terrestrial sediment: How might climate change have affected erosion rates? Annual Review of Earth and Planetary Sciences, 32(1), 67–89. https://doi.org/10.1146/annurev.earth.32.091003.143456.

Morley C.K., 2002. A tectonic model for the Tertiary evolution of strike-slip faults and rift basins in SE Asia. Tectonophysics, 347(4), 189–215. https://doi.org/10.1016/S0040-1951(02)00061-6.

Morley C.K., 2016. Major unconformities/termination of extension events and associated surfaces in the South China Sea (East Sea)s: Review and implications for tectonic development. Journal of Asian Earth Sciences, 120, 62–86. https://doi.org/10.1016/j.jseaes.2016.01.013.

Morley C.K., 2017. The impact of multiple extension events, stress rotation and inherited fabrics on normal fault geometries and evolution in the Cenozoic rift basins of Thailand. In: Childs C., Holdsworth R.E., Jackson C.A.-L., Manzocchi T., Walsh J.J., Yielding G. (Eds): The Geometry and Growth of Normal Faults. Geological Society, London, Special Publications, 439, 413–445.

Morley C.K., Racey A., 2016. Tertiary Stratigraphy. In: Ridd M.F., Barber A.J. and Crow M.J. (Eds.): The Geology of Thailand, Geological Society, London, 223–271.

Morley C.K., Westaway R., 2006. Subsidence in the super-deep Pattani and Malay basins of Southeast Asia: A coupled model incorporating lower-crustal flow in response to post-rift sediment loading. Basin Research, 18(1), 51–84. https://doi.org/10.1111/j.1365-2117.2006.00285.x.

Morley R.J., 2012. A review of the Cenozoic palaeoclimate history of Southeast Asia. In: Gower et al. (Eds): Biotic Evolution and Environmental Change in Southeast Asia. Cambridge University Press, Cambridge, 79–114. https://doi.org/10.1017/CBO9780511735882.006.

Morley R.J., Tung N., Dung B.V., Kullman A.J., Bird R.T., 2019. A Revised Chronostratigraphy for the Cuu Long Basin, based on the interpretation of climate-driven depositional cycles during the Late Eocene/Oligocene and VIM depositional cycles during the Mio-Pliocene. Seapex 2nd-5th April 2019, Singapore, 4p.

Ngah K., Madon M., Tjia H.D., 1996. Role of pre-Tertiary fractures in formation and development of the Malay and Penyu basins. In: Hall R., Blundell D. (Eds.), Tectonic Evolution of Southeast Asia: Geological Society Special Publication, 106, 281–289. https://doi.org/10.1144/GSL.SP.1996.106.01.18.

Nguyen T.-A., Fyhn M.B.W., Kristensen J.Å., Nielsen L.H., Thomsen T.B., Keulen N., Lindström S., Boldreel L.O., 2021. Provenance of the Phuquoc Basin fill, southern Indochina: Implication for Early Cretaceous drainage patterns and basin configuration in Southeast Asia. Gondwana Research, 98, 166–190. https://doi.org/10.1016/j.gr.2021.03.014.

Nytoft H.P., Fyhn M.B.W., Hovikoski J., Rizzi M., Abatzis A., Tuan H.A., Tung N.T., Huyen N.T., Cuong T.X., Nielsen L.H., 2020. Biomarkers of Oligocene lacustrine source rocks, Beibuwan-Song Hong basin junction, offshore northern Vietnam. Marine and Petroleum Geology, 114, 104196, https://doi.org/10.1016/j.marpetgeo.2019.104196.

Olson C., Dorobek S., 2000. Timing and tectonic implications of structural inversion in the Nam Con Son Basin and adjacent areas, southern South China Sea (East Sea). Abstracts with Program- Geological Society of America, 32(7), 237.

Petersen H.I., Mathiesen A., Fyhn M.W.F., Dau N.T., Bojesen-Koefoed J.A., Nielsen L.H., Nytoft H.P., 2011. Modeling of petroleum generation in the Vietnamese part of the Malay Basin using measured

kinetics. AAPG Bulletin, 95, 509–536, https://doi.org/10.1306/09271009171.

Petersen H.I., Sherwood N., Mathiesen A., Fyhn M.B.W., Dau N.T., Russell N., Bojesen-Koefoed J.A., Nielsen L.H., 2009. Application of integrated vitrinite reflectance and FAMM analyses to solve problems in thermal maturity assessment of the northeastern Malay Basin, offshore SW Vietnam: Implications for petroleum prospectivity evaluation. Marine and Petroleum Geology, 26, 319–332, https://doi.org/10.1016/j.marpetgeo.2008.04.004.

Phoosongsee J., Morley C., Ferguson A.J., 2019. Quantitative interpretation of seismic attributes for reservoir characterization of Early-Middle Miocene syn- and post-rift successions (Songkhla Basin, Gulf of Thailand) Marine and Petroleum Geology, 109, 791–807.

Pubellier M., Morley C.K., 2014. The basins of Sundaland (SE Asia): Evolution and boundary conditions. Marine and Petroleum Geology, 58, 555–578.

Rizzi M., Fyhn M.B.W., Schovsbo N.H., Korte C., Hovikoski J., Olivarius M., Thomsen T.B., Keulen N., Thuy N.T.T., Hoang B.H., Dung B.V., Toan D.M., Abatzis I., Nielsen L.H., 2020. Hinterland Setting and Composition of an Oligocene Deep Rift-lake Sequence, Gulf of Tonkin, Vietnam: Implications for Petroleum Source Rock Deposition. Marine and Petroleum Geology, 111, 496–509. https://doi.org/10.1016/j.marpetgeo.2019.08.022.

Sangree J.B., Widmier J.M., 1977. Seismic stratigraphy and global changes of sea level, Part 9: Seismic interpretation of clastic depositional facies. In: Payton, C.E. (Ed.), Seismic Stratigraphy-Application to Hydrocarbon Exploration. AAPG Memoir, 26, 165–184.

Smith M., Chantraprasert S., Morley C.K., Cartwright I., 2007. Structural geometry and timing of deformation in the Chainat duplex, Thailand. Geological Society, London, Special Publications, 290(1), 305–323. https://doi.org/10.1144/SP290.11

Smith W.J., Bui H., Handschy J.W., Hai V.T., Cuong T.X., Tung N.T., 2019. Tectonic evolution and regional setting of the Cuu Long Basin, Vietnam. Tectonophysics, 757, 36-57. https://doi.org/10.1016/j.tecto.2019.03.001.

Tapponnier P., Peltzer G., Armijo R., 1986. On the mechanics of the collision between India and Asia. Coward M.P., Ries A.C. (Eds.): Collision Tectonics. Geological Society, London, Special Publications, 9, 115–157.

Taylor B., Hayes D.E., 1983. Origin and history of the South China Sea (East Sea) Basin. In: Hayes D.E.(Ed.): The Tectonic and Geologic Evolution of Southeast Asian Seas and Islands. Geophysical Monograph, 23, 89–104.

Tjia H.D., 1994. Inversion tectonics in the Malay Basin: evidence and timing of events. Geol. Soc. Malaytlia, Bulletin, 56, 119–126.

Tjia H.D., Liew K.K., 1996. Changes in tectonic stress field in northern Sunda Shelf basins. Geological Society, London, Special Publications, 106(1), 291–306. https://doi.org/10.1144/GSL.SP.1996.106.01.19.

Vinh L.N., Cable G., 1997. B-KL-1X “Kim Long”, geological completion report, block B, offshore Vietnam. Unocal Vietnam Exploration, Ltd., HCMC, Vietnam.

Vinh L.V., Cable G., 2001. B-KL-4X “Golden Dragon - Kim Long”, geological completion report, block B, offshore Vietnam. Unocal Vietnam Exploration Ltd., HCMC, Vietnam.

Waight T., Fyhn M.B.W., Thomsen T.B., Tri T.V., Nielsen L.H., Abatzis I., Frei D., 2021. Permian to Cretaceous granites and felsic volcanics from SW Vietnam and S Cambodia: Implications for tectonic development of Indochina. Journal of Asian Earth Sciences, 219, 104902, https://doi.org/10.1016/j.jseaes.2021.104902.

Wei G., X.-H. Li, Y. Liu, L. Shao, X. Liang, 2006. Geochemical record of chemical weathering and monsoon climatechange since the early Miocene in the South China Sea (East Sea), Paleoceanography, 21, PA4214. Doi: 10.1029/2006PA001300.